


Article

Hydrochemical Characteristics and the Relationship between Surface and Groundwater in a Typical ‘Mountain–Oasis’ Ecosystem in Central Asia

Congjian Sun ^{*} , Shiyu Wang and Wei Chen

School of Geographical Science, Shanxi Normal University, Taiyuan 030031, China; wangshiyuzuibang@sina.com (S.W.); wan_xin_chen@126.com (W.C.)

* Correspondence: suncongjian@sina.com

Abstract: Water environment monitoring is an important way to optimize the allocation and sustainable utilization of regional water resources and is beneficial for ensuring the security of regional water resources. In order to explore hydrochemical distributions in a mountain–oasis ecosystem in Central Asia, surface water and groundwater samples from the Kaidu River basin were collected over four seasons. pH values, major ions, total dissolved solids (TDS) and stable isotopes were determined during the period from 2016 to 2017. The results showed: (1) that most water bodies in the study areas were mildly alkaline and that hydrochemical distributions showed significant seasonal and spatial variation; (2) that δD and $\delta^{18}O$ in surface water and groundwater showed enrichment in summer and autumn and poverty in spring and winter, with higher $\delta^{18}O$ values appearing in the oasis area and lower $\delta^{18}O$ values appearing in the mountain area; (3) that most of the water bodies in the study areas were of $HCO_3^-Ca^{2+}$ type, with the hydrochemical types of groundwater presenting obvious spatial inconsistency relative to surface water; (4) that rock weathering was the main factor controlling hydrochemical composition in the study areas and that human activities had an influence on the groundwater environment in the oasis area; (5) and that surface water–groundwater interactions also displayed spatial inconsistency, especially in summer. The interaction between river water and groundwater was more obvious in the traditional oasis area, especially in spring and summer. The results will be important for regional water resource management and sustainable water utilization.

Keywords: hydrochemistry; stable isotopes; spatial–temporal variation; surface water and groundwater relationship



Citation: Sun, C.; Wang, S.; Chen, W. Hydrochemical Characteristics and the Relationship between Surface and Groundwater in a Typical ‘Mountain–Oasis’ Ecosystem in Central Asia. *Sustainability* **2022**, *14*, 7453. <https://doi.org/10.3390/su14127453>

Academic Editor: Venkat Sridhar

Received: 26 May 2022

Accepted: 15 June 2022

Published: 18 June 2022

Publisher’s Note: MDPI stays neutral with regard to jurisdictional claims in published maps and institutional affiliations.



Copyright: © 2022 by the authors. Licensee MDPI, Basel, Switzerland. This article is an open access article distributed under the terms and conditions of the Creative Commons Attribution (CC BY) license (<https://creativecommons.org/licenses/by/4.0/>).

1. Introduction

Water is one of the most precious natural resources for human survival and is an irreplaceable strategic resource for national economic development. The shortage of water resources has become a “bottleneck” factor restricting economic growth and social progress in many countries and regions [1–3]. As an important part of and the most active element in the natural environment, water plays a decisive role in the process of natural evolution. As the most important restrictive resources in arid inland areas, water resources are directly related to the sustainable development of regional economies, societies and ecological environments, particularly in arid inland areas of Central Asia [1,2]. The relatively odious climate environment (characterized by such factors as fluctuating temperature, scarce precipitation and strong evaporation) leads to unequal spatial and temporal distributions of water resources in inland areas of Central Asia [3], which further increases the disparity between supply and demand for regional water resources. With the increases in population, economic growth, social progress and the development of industrial and agricultural production and especially with the rise of modern industry and the expansion of cities, human demand for water resources is increasing [4]. In order to meet the growing demand for water, human beings have taken various measures to expand the development of

water resources. This has achieved short-term economic benefits but it has also had a serious impact on the ecological environment. The problems of water shortage and water insecurity are becoming more and more serious, especially in inland areas of Central Asia [4]. Nowadays, groundwater contamination is a critical issue in many countries, since it is directly related to water usage, food safety, and human health [5]. Evaluation of water quality is of great importance in the management of water supplies [6]. Water quality is considered a severely limiting factor in relation to public health and economic development [7]. However, studies of typical mountain–oasis ecosystems in Central Asia are relatively underdeveloped. Under the combined influence of regional climate change and large-scale human activities, it has become important for regional sustainable development to explore hydrochemical compositions and relationships in varietal water bodies, especially in Central Asia [4,8].

In arid areas of Central Asia, investigation of the spatial distribution of dissolved ion concentrations in multiple water bodies is important for understanding the origin, migration, and evolution of groundwater salinity, which is helpful in further understanding the hydrological circulation process in arid areas [9]. In addition, monitoring the hydrochemical composition of surface water in arid areas is essential for improving recognition of water and sediment discharge and variation in global hydrochemical flux [10]. Therefore, hydrochemical information for various water bodies can reflect the basic characteristics of inland river basins, which is of great significance for maintaining regional water security, the rational utilization of water resources and sustainable development [11]. In the past several decades, hydrochemical information on inland river systems in Central Asia [11–13], North Africa [14] and arid inland areas of China [15–18] has been fully recorded and analyzed. The projection of temporal and spatial distribution characteristics of river water chemistry provides unique insights into the protection of the ecological environment, the rational utilization of water resources and the hydrological function of inland river basins.

In 1944, Piper created the Piper ternary diagram for use in the identification of hydrochemical composition types [19]. This method plays an important role in distinguishing hydrochemical types in India [1,10], Northeast China [20,21] and Northwest China [22–24]. In arid inland areas of China, many recent studies have investigated the variation in the temporal and spatial distributions of hydrochemical compositions (e.g., in the Hexi Corridor Area [25], the Tarim inland river basin [26] and the northern Xinjiang inland river basin [27]) and indicated that groundwater and river water in these regions is alkaline. In the arid inland areas of China, rock weathering, evaporation–crystallization processes and human activities are likely linked to hydrochemical variation in regional water bodies [28]. In the Hexi Corridor Area of China, a number of studies have analyzed the characteristics of the water environments among multiple water bodies in the Shiyang River, Heihe River and Shule River basins. These studies indicated that the main ions in this region were Ca^{2+} and HCO_3^- and that rock weathering had a significant influence on regional hydrochemical distribution [29–31]. Downstream of the Tarim River Basin, the results of groundwater hydrochemical monitoring in the oasis area suggested that Na^+ , Mg^{2+} , and HCO_3^- [26] were relatively enriched and that the chemical composition of groundwater was mainly controlled by rock dominance and evaporation–crystallization processes. In Northern Xinjiang, surface water was mostly of the Ca^{2+} - HCO_3^- type, which is consistent with studies of the Urumqi River basin [27]. In the Urumqi basin, the hydrochemical process of the slowflow period was controlled by water–rock interactions, while precipitation processes had a significant influence on the hydrochemical processes in the quickflow period. These studies further improved understanding of regional hydrological processes in inland arid areas of Central Asia.

Mountains and oases are the basic geographical landscapes of inland arid areas in Central Asia and their combinations are referred to as mountain–oasis systems (MOSs) [32]. Not only is this a regional geological and topographical framework, it also determines the climatic conditions, ecosystem model, and human activities in Central Asia [33]. Water resources are considered as important restrictive resources and variation driving factors

of the MOS, and its environmental change often leads to significant variation in the MOS. In Central Asia, some projects have evaluated the ecological service function, ecological security, the landscape and land use change of the MOS [34,35]. However, the spatial-temporal variation mechanism of hydrochemical of surface water and groundwater in the MOS of Central Asia is still unclear, especially in the southern Tianshan Mountains of China. The Kaidu river basin is a typical mountain–oasis ecosystem in Tianshan Mountains, and its oasis area is of great significance to the economic and social development of the whole South Tianshan Mountains [36]. Recently, with the increase of population, the expansion of oasis scale and the unreasonable utilization of water resources, the regional water environment has deteriorated, and the relationship between surface water and groundwater has become increasingly complex, which seriously threatens the security of regional ecological environment and the sustainable development of economy and society [37]. It is urgent and necessary to systematically analyze and explore regional water environment of this study area.

Therefore, this research project systematically analyzes and reveals the hydrochemical characteristics of surface water and groundwater in the Kaidu river basin based on four whole basin sampling. The main objectives of this study are: (1) to analyze the spatial and seasonal variation of main ions and isotopes of surface water and groundwater, (2) to determine hydrochemical types of various water bodies, (3) to explore mainly controlling mechanism for regional water environment, and (4) to identify the transformation relationship between regional surface water and groundwater. The results of this project will further enrich the understanding of regional hydrological process of mountain–oasis ecosystem in the alpine region of Central Asia, and provide a certain reference for the effective management and rational utilization of water resources in the study area.

2. Materials and Methods

2.1. Study Area

The study area is a typical mountain–oasis ecosystem in Central Asia, which is located in the south slope of the Central Tianshan Mountains in Xinjiang, China (between $41^{\circ}48'–42^{\circ}16'$ N and $86^{\circ}08'–87^{\circ}26'$ E) and covers an area of 5941.49 km² (Figure 1) [38]. The annual temperature of the study area is 7.9 °C, and average annual precipitation is less than 150 mm. There are significant differences in temperature and precipitation between mountainous and oasis areas in the study area. Based on the Koppen classification of climate, the oasis area of the study area belongs to subtropical temperature cold desert climate pattern (B Wk) of the arid desert climate pattern (B W), the average annual temperature is lower than 18 °C and the potential evaporation capacity is greater than the annual precipitation (about 100 mm). In the mountain area, the climate pattern belongs to the alpine cold climate, where average annual precipitation is larger than the oasis area. The temperature and precipitation presented obviously vertical belt distribution [39,40]. The main rivers in the study area include the Kaidu River, the Huanghuigou River and the Qingshui River, which all originate from the Tianshan Mountains and are supplied by alpine precipitation, bedrock fissure groundwater and glacier/snow melt water. Oasis region of this study area, with a total farmland area of 2583 km², is an important gathering area of population, industry and irrigated agriculture in Xinjiang Province, which is suitable for pepper, tomato, corn, wheat and other crops [41]. Recently, continuous expansion of oasis area caused by the rapid increase of regional population, the unsustainable use of regional water and land resources, and the adverse effects caused by regional climate change have led to the increasingly fragile ecological environment and the continuous deterioration of water environment in the study area.

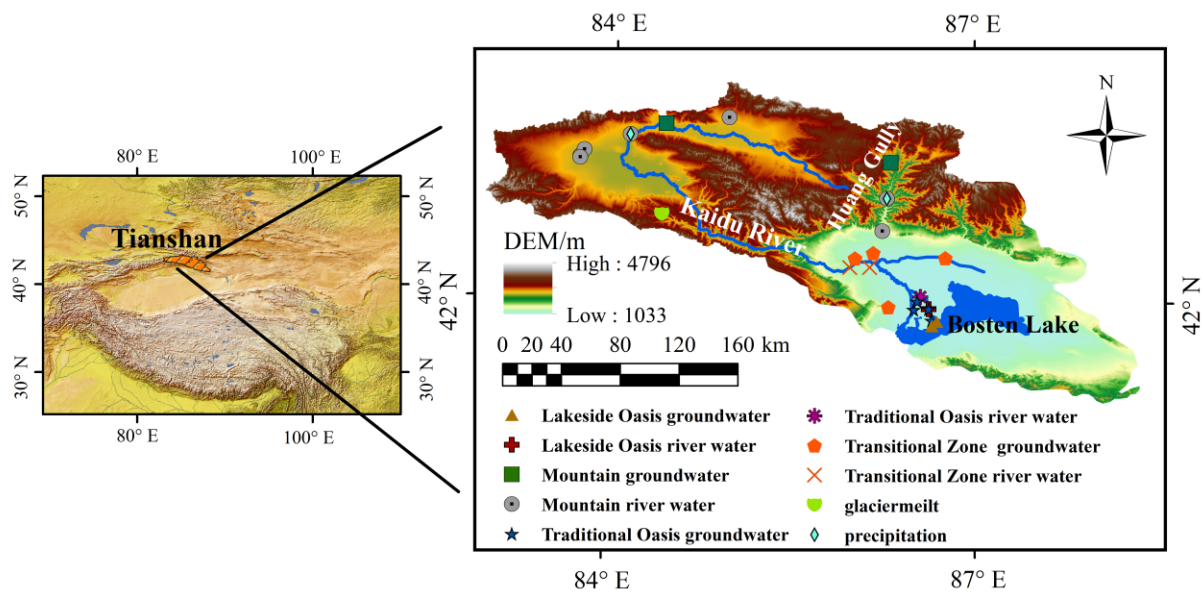


Figure 1. Location of the study area and distribution of samples.

2.1.1. Climate Pattern

Climate change has been confirmed to have significant effects on the regional water environment and hydraulic connections [39]. Over the past decade, mainly climate factors in the study area fluctuated significantly (Figure 2). On the whole, annual temperature in the study area showed an increasing trend, and precipitation presented some fluctuation, while the potential evaporation showed a relatively smooth trend. Inconsistent inter-annual variation was observed between the mountain areas and the oasis areas. The temperature in the mountainous area was relatively lower than that of the oasis area, while increasing trend of the mountainous area was higher than that of the oasis area, especially since 1998 (the increased temperature in the mountain area caused more ice and snow melt water recharge river water and groundwater, further influence regional water environment). The precipitation of the oasis areas was generally higher than that of the mountainous areas, but the increase rate of precipitation of the mountainous areas was more obviously than that of the oasis areas, which will bring more supply water resource to the surface/ground water. Potential evaporation showed inconsistent variability trend with temperature and precipitation. Potential evaporation in the mountainous areas had not significantly variability during past 60 years, while potential evaporation in the oasis areas was higher than that in the mountainous areas, especially in the last 20 years [34,35].

2.1.2. Social and Economic Characteristics

With the rapid increase in population, food pressure has led to significant changes in regional land–use and land–cover (LUCC) patterns. The main land use types in the study area were grassland and water area in the mountains area. In the oasis region, cultivated land, industrial land and some grassland occupied large proportion. The LUCC in the study area indicated (Figure 2d), the land use types in the mountainous area presented stable trend, while the LUCC of the oasis area shown obviously variation. In the Oasis region, some grassland and forests were change to cultivated land, and the oasis area expanded nearly three times during past 20 years (Figure 2).

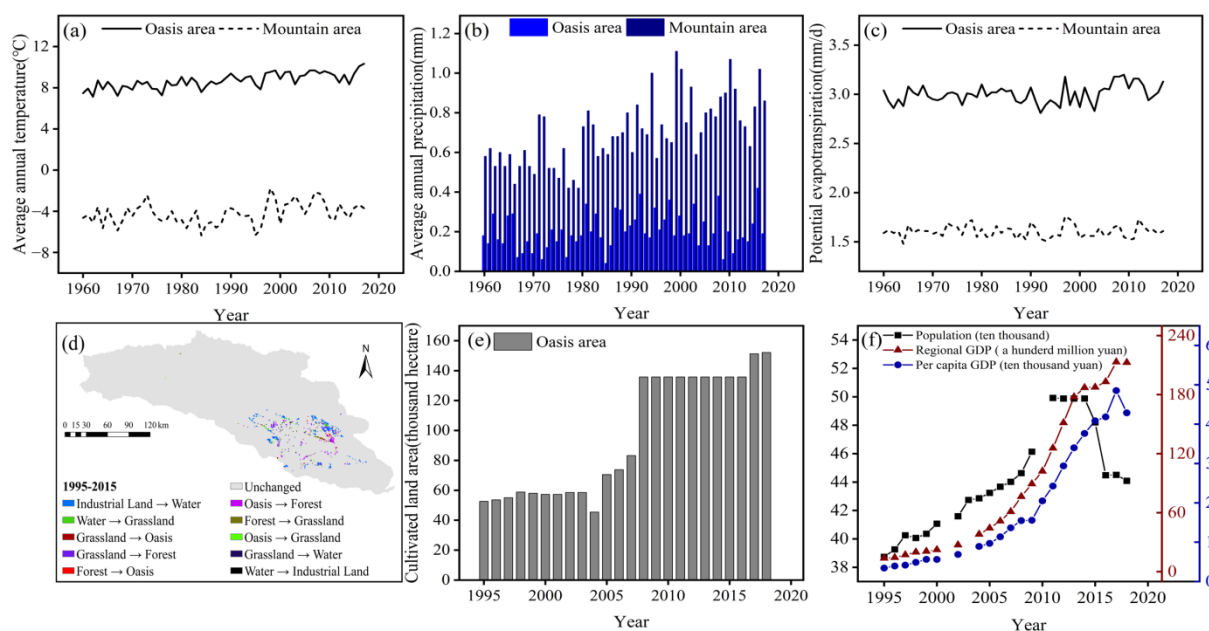


Figure 2. Characteristics of economic, social and climatic factors in the study area. (a) average annual temperature in mountainous and oasis areas; (b) average annual precipitation in mountainous and oasis areas; (c) potential evapotranspiration in mountainous and oasis areas; (d) land–use and land–cover change in mountainous and oasis areas; (e) changes in oasis area from 1995 to 2018; (f) population and GDP changes in the study area from 1995 to 2018).

2.2. Sample Collection and Analysis

2.2.1. Sample Collection

To reveal spatiotemporal variations in regional water environment in the study area, 119 surface water and groundwater samples were collected in the mountain and oasis areas during April 2016 (representing spring), July 2016 (summer), September 2016 (autumn) and January 2017 (winter), respectively. There were 48 groundwater samples and 46 river water samples, 13 precipitation samples, and 12 glacier water samples. In order to present the hydrochemical spatial variations in more detail, this study divided oases region into three types: transition zone (oasis and desert transition area), oasis area (traditional oasis area) and lakeside area (newly opened oasis near Bosten Lake) according to previous studies [28].

Fixed sampling points were selected for sampling river water and groundwater samples in different seasons. Due to the traffic accessibility in the study area is poor, the selected sample points need to ensure that water samples can be collected throughout the year. The details of sampling location are shown in Table 1. In this study, shallow groundwater (<20 m) was selected as the groundwater sampling point, flowing natural water surface was selected as the river water, precipitation samples collected from the hydrological station, and glacier samples were collected from the glacier observation station in the Tianshan Mountains. Isotopic water samples were stored in 5 mL glass bottles and immediately sealed with parafilm sealing membrane to reduce evaporation. Before the hydrochemical river sample collection, the plastic sampling bottle (500 mL) was cleared three times with the collected samples. In order to avoid contact the water sample with the atmosphere during the sampling of glacier water, the surface part of the glacier was always removed. All groundwater samples were collected after the field parameters were stable to eliminate the influence of stagnant water. Water samples for ion concentration analysis were collected in plastic bottles that were sealed immediately after collection and stored at $-18\text{ }^{\circ}\text{C}$. Prior to analysis, samples were transferred into a refrigerator at $4\text{ }^{\circ}\text{C}$ to thaw gradually so that evaporation did not occur.

Table 1. Information of surface and ground water samples in the study area.

Type of Sample	Regions	Samples	Longitude	Latitude	Number of Samples	
Surface water	Traditional oasis area	O1	86.55	42.05	4	
		Lakeside area	O2	86.62	41.98	4
	Transition zone	O3	86.14	42.23	4	
		O4	85.97	42.23	4	
	River water	Mountain area	M1	86.24	42.45	4
			M2	86.27	42.65	4
			M3	84.95	43.13	4
			M4	84.95	43.13	4
			M5	84.13	43.01	4
			M6	83.72	42.87	4
			M7	83.75	42.91	3
			M8	83.72	42.86	3
	Precipitation		P1	86.27	42.65	7
	Glacier water		P2	84.13	43.01	6
			G1	84.41	42.53	12
Groundwater	Traditional oasis area	La1	86.65	41.91	4	
		La2	86.50	41.97	4	
		La3	86.53	42.02	4	
		La4	86.62	41.98	4	
	Lakeside area	Lb1	86.69	41.90	4	
		Lb2	86.65	41.87	4	
		Lc1	86.76	42.29	4	
	Transition zone	Lc2	86.16	42.32	4	
		Lc3	86.01	42.29	4	
		Lc4	86.29	41.99	4	
		MG1	86.30	42.87	4	
	Mountain area	MG2	84.43	43.09	4	

2.2.2. Sample Testing and Laboratory Analysis

The $\delta^{18}\text{O}$ and δD values and major ions values of water samples were measured at the State Key Laboratory of Desert and Oasis Ecology, Xinjiang Institute of Ecology and Geography, Chinese Academy of Sciences. $\delta^{18}\text{O}$ and δD values were measured by the Liquid Water Isotope Analyzer (Model DLT-100, Los Gatos Research, San Jose, CA, USA), its accuracy levels were 0.1‰ and 0.3‰, respectively. The measurement results were reported by the Vienna Standard Mean Ocean Water (V-SMOW). Dual-column instrument (Dionex DX-100, Dionex, Sunnyvale, CA, USA, analytical errors were: Ca^{2+} (± 0.4 mg/L), Mg^{2+} (± 0.7 mg/L), Na^+ (± 0.1 mg/L), K^+ (± 0.1 mg/L), Cl^- (± 0.1 mg/L), SO_4^{2-} (± 0.3 mg/L), HCO_3^- (± 0.3 mg/L)) was used to measure the major ion concentration of surface and ground water. Some parameters (pH, water temperature and the total dissolved solids (TDS)) were tested in situ using a portable multiparameter instrument (Manta 2) adjusted with a standard solution.

2.3. Analysis Method

The piper ternary diagram, Gibbs diagram, and environmental isotope tracing methods are common methods to explore the hydrochemical characteristics of different water bodies and the influence of main weathering processes [18]. The EMMA (end member mixing analysis) method was applied in research to identify the relationship between different water bodies [8]. The three-component method [8] was used to calculate the ratios

of interaction between groundwater and various recharging water sources. The method can be described by the following equations:

$$Q = \sum_{m=1}^n Q_m$$

$$QC_Q^b = \sum_{m=1}^n Q_m C_m^b \quad b = 1, \dots, k \quad (1)$$

where Q is total groundwater discharge, Q_m is the discharge of component m , and C_m^b is the tracer b incorporated into the component m .

3. Results

3.1. General Hydrochemical Characteristics of the Study Area

3.1.1. pH and TDS

In this study, the range of pH values in river water samples were 7.44~8.30, which indicated that the river water in the study area was alkaline and showed significant seasonal variation. The average pH value of river water showed an obvious order: winter (8.16) > spring (8.01) > autumn (7.87) > summer (7.80). The river water pH displayed higher values in winter and spring and lower values in summer and autumn. In winter and spring, Higher pH value was associated with less precipitation and concentrated river water concentration, and the dilution effect of summer precipitation and snow melting water were the main reasons for the lower pH of the river water [8]. The rivers samples of the mountainous areas and oasis areas presented inconsistent seasonal variation patterns. As for the oasis region, pH value of river water showed an order of summer > autumn > winter > spring in the traditional oasis area. The lakeside area was winter > summer > autumn > spring, while the transition zone was summer > winter > spring > autumn. However, in the mountain area, the order of pH seasonal variation was winter > spring > autumn > summer. The pH value of river water also showed significant spatial inconsistency. The pH value of river water in the transition zone was generally higher than that in other areas. Comparing different seasons, in the spring, the spatial variation of river pH in the study area was as follows: the transition zone > the mountainous area > the traditional oasis area > the lakeside area. In summer and autumn, the performance was: the transition zone > the traditional oasis area > the lakeside area > the mountainous area. In winter, the performance was: the transition zone > the mountain area > the lakeside area > the traditional oasis area.

The pH values of groundwater samples ranged from 7.75 to 8.28, indicating that the groundwater in the study area was also alkaline. The average pH value of groundwater showed a seasonal order of winter (8.11) > spring (8.01) > summer (7.97) > autumn (7.81). The seasonal variation of groundwater pH in most areas of the study area was winter > spring > summer > autumn, except for the pH of groundwater in the transition zone (winter > summer > spring > autumn). As for spatial variation, the groundwater pH of the oasis area was generally higher than that of the mountain area (except in winter). The higher groundwater pH values in the oasis area are closely linked to the local irrigation agriculture development, and the irrigation water washes salt from surface soil into the groundwater system [42]. In the oasis area, the pH of groundwater of the transition zone and lakeside area were relatively higher than that of the transition zone throughout whole year. The pH values of precipitation samples in the study area ranged from 5.94 to 7.38 and showed a seasonal order of spring (6.52) > autumn (6.43) > summer (6.18). The pH values of glacier water samples ranged from 6.73 to 7.68. The average pH values of glacier water samples showed a seasonal order of spring (7.38) > summer (6.78) > autumn (6.87).

The TDS values of river water samples in the study area ranged from 64.45 to 798.00 mg·L⁻¹. The average value of river water TDS showed an obvious seasonal order of winter (337.88 mg·L⁻¹) > spring (327.62 mg·L⁻¹) > autumn (273.36 mg·L⁻¹) > summer (236.82 mg·L⁻¹). Lower TDS values was associated with the dilution effect of summer precipitation and snow melting water. The TDS value of river water in the traditional oasis

area showed a order of spring > winter > autumn > summer. The variation trends of the lakeside area and transition zone were similar, which seasonal order were winter > spring > autumn > summer. The variation trend of TDS value of river water in the mountainous area was similar as that in the traditional oasis area. The spatial distribution of river TDS was also inconsistent. Among them, the TDS value of river water in the lakeside area was generally higher than that in other areas, while the TDS value of river water in the mountainous area was relatively lower than that in the oasis area. The higher river water TDS levels in the lakeside area may be closely related to the interaction between river water and lake water, which has a higher TDS value [43,44]. In addition, in the oasis area, the TDS value of river water in spring, summer and autumn presented a relatively similar spatial distribution pattern, that was, the lakeside area > the traditional oasis area > the transition zone, while the TDS value in the transition zone in winter was significantly inconsistent with that in other areas.

The TDS values of groundwater samples in the study area were in the range of 119.58–1077.00 mg·L⁻¹. The seasonal variation of TDS of groundwater in the study area was similar to that of river water. In the traditional oasis area, the TDS value of groundwater was winter (606.32 mg·L⁻¹) > autumn (482.76 mg·L⁻¹) > spring (522.00 mg·L⁻¹) > summer (451.09 mg·L⁻¹). In the lakeside area, the TDS value of groundwater was winter > spring > summer > autumn. In the transition zone, the TDS of groundwater presented spring > winter > summer > autumn. The seasonal variation of groundwater TDS in mountainous area was the same as that in oasis area, which was winter > spring > autumn > summer. For spatial distribution, the TDS value of the mountainous area was relatively lower than that of the oasis regions (irrigation agriculture has an obvious influence on the groundwater system [45]), while the oasis regions showed an obvious spatial variation of the groundwater TDS was the transition zone > lakeside area > traditional oasis area in spring and summer.

As for precipitation, TDS values of precipitation samples ranged from 18.30 to 141.40 mg·L⁻¹ and included 56.20 to 141.40 mg·L⁻¹ in spring, 18.30 to 75.20 mg·L⁻¹ in summer and 70.60 to 130.10 mg·L⁻¹ in autumn. The average TDS values of precipitation samples showed a seasonal order of autumn (104.07 mg·L⁻¹) > spring (88.48 mg·L⁻¹) > summer (37.72 mg·L⁻¹). The TDS value of glacier water ranges from 60.00 to 95.00 mg·L⁻¹, with relatively weak seasonal fluctuation. The average TDS value of glacier water showed a seasonal order of summer (70.00 mg·L⁻¹) > autumn (67.09 mg·L⁻¹) > spring (66.70 mg·L⁻¹).

3.1.2. Major Ions Concentrations

The average, maximum, and minimum values of the content of inorganic ions in all samples are presented in Table 2. In river water samples, the variation of ion concentration shows significant seasonal variation. In general, HCO₃⁻ and Ca²⁺ were the main anions and cations, accounting for 72% and 60% of the total anions and cations, respectively.

In river water samples, the fluctuation range of ions is relatively small, which is related to the relatively stable runoff composition pattern in this study area. Among them, the fluctuation of bicarbonate ions and calcium ions in mountain river samples are relatively obviously, which mainly closely related to the interaction between water and rocks in the process of alpine precipitation and melting water replenishing surface river water. Significant fluctuations in river water Cl⁻ was observed in the lakeside oasis area and similar phenomena were observed in the SO₄²⁻, Na⁺ of the river water samples. The fluctuation of ion values in the river water samples of Lakeside area may be related to the interaction between the lake and the river.

Table 2. Statistical summary of hydrochemical variables of surface and groundwater in different seasons.

Season	Type		pH	TDS (mg/L)	Ca ²⁺ (mg/L)	Mg ²⁺ (mg/L)	Na ⁺ (mg/L)	K ⁺ (mg/L)	HCO ₃ ⁻ (mg/L)	Cl ⁻ (mg/L)	SO ₄ ²⁻ (mg/L)
Spring	groundwater	max	8.22	771.00	64.60	26.37	100.48	5.54	305.95	64.58	174.13
		min	7.77	204.00	4.31	2.15	4.96	0.94	111.87	2.85	10.99
		ave	8.01	522.00	35.07	12.91	49.01	3.01	193.94	37.36	72.15
	river water	max	8.23	444.00	68.83	14.33	16.82	2.45	217.40	23.62	63.42
		min	7.59	255.00	33.32	7.39	6.74	1.50	78.13	6.13	15.93
		ave	8.01	327.62	49.82	10.74	11.49	2.46	180.83	11.31	39.16
	precipitation	max	7.38	141.40	17.74	1.43	6.18	2.87	52.00	17.10	18.94
		min	6.17	56.20	10.32	0.39	1.09	0.76	29.41	7.13	4.20
		ave	6.52	88.48	15.36	0.82	2.64	1.31	37.85	12.42	7.96
	glacier water	max	7.68	71.10	7.89	0.40	2.31	2.38	50.53	3.16	1.80
		min	7.07	62.30	4.12	0.35	0.76	0.69	31.53	0.86	1.26
		ave	7.38	66.70	6.00	0.38	1.53	1.54	41.03	2.01	1.53
Summer	groundwater	max	8.10	645.00	99.91	31.06	106.69	5.01	313.89	101.06	201.72
		min	7.75	137.90	18.93	5.43	6.23	0.69	109.40	2.74	11.24
		ave	7.97	451.09	50.45	14.93	53.37	2.73	189.22	42.19	82.88
	river water	max	8.19	353.00	56.77	11.71	10.94	1.86	188.65	14.64	54.32
		min	7.44	114.80	13.99	1.34	0.68	0.44	49.61	0.82	8.98
		ave	7.80	236.82	38.67	7.35	5.90	1.23	137.54	5.44	27.15
	precipitation	max	6.73	75.20	11.63	0.55	1.02	1.27	41.43	15.47	3.34
		min	5.94	18.30	2.85	0.13	0.09	0.21	11.79	0.93	1.02
		ave	6.18	37.72	5.75	0.25	0.41	0.67	22.66	5.21	1.81
	glacier water	max	6.84	95.00	4.44	0.58	0.05	0.63	35.92	2.26	3.49
		min	6.73	60.00	2.62	0.33	0.00	0.14	23.95	1.16	1.27
		ave	6.78	70.00	3.07	0.42	0.03	0.29	32.09	1.51	1.91
Autumn	groundwater	max	7.92	1049.35	81.41	28.34	219.32	7.57	182.10	121.91	423.75
		min	7.70	149.50	15.21	4.87	5.37	0.61	110.70	2.61	12.16
		ave	7.81	482.76	41.44	13.60	70.96	2.68	159.57	50.38	113.73
	river water	max	7.99	434.00	63.10	16.05	36.66	3.17	275.44	20.34	60.50
		min	7.69	142.10	31.42	2.91	5.29	0.80	112.00	1.74	8.41
		ave	7.87	273.36	46.45	10.48	11.80	1.64	170.40	9.09	36.87
	precipitation	max	6.47	130.10	3.88	0.31	0.89	3.06	63.58	49.81	11.49
		min	6.40	70.60	3.76	0.14	0.16	0.45	52.59	6.84	1.68
		ave	6.43	104.07	3.81	0.21	0.48	1.59	58.77	31.01	7.20
	glacier water	max	6.91	78.34	3.95	0.46	0.31	0.56	35.66	1.83	2.52
		min	6.84	60.84	3.05	0.34	0.12	0.32	34.00	1.28	1.41
		ave	6.87	67.09	3.36	0.39	0.22	0.41	34.70	1.45	1.82
Winter	groundwater	max	8.23	1077.30	66.05	60.68	113.62	5.49	314.23	118.61	207.06
		min	7.97	119.58	19.91	2.14	6.27	1.88	147.47	9.77	38.63
		ave	8.11	606.32	44.92	24.22	55.56	3.62	225.33	53.12	100.17
	river water	max	8.30	798.00	67.56	34.76	17.54	2.35	214.63	24.29	69.75
		min	7.91	64.45	21.41	0.52	2.52	0.37	49.87	0.0	7.49
		ave	8.16	337.88	44.19	11.53	7.85	1.61	170.83	16.07	32.82

In precipitation, HCO₃⁻ and Ca²⁺ were the main anions and cations, accounting for 66% and 73% of the total anions and cations. As for glacier water samples, the total mass of HCO₃⁻ and Ca²⁺ were the main anion and cation, accounting for 90% and 70% of the total anions and cations. In comparison, the ion variability range of precipitation and glacier samples were relatively smaller and their mean values were smaller than in river water and groundwater samples.

As for groundwater, the total mass of cations was mainly Na⁺, accounting for more than 40% of the total mass of cations especially in the Oasis region, while Ca²⁺ was the second largest substantive cation. The relatively high sodium values of groundwater in the oasis region are associated with salt rinsing and flushing dissolution during agricultural irrigation, where agricultural irrigation water washes the salts in the surface soil and seeps into the groundwater. HCO₃⁻ and SO₄²⁻ were the main anions in groundwater samples. On the whole, the ion concentration fluctuation of groundwater was remarkable greater than that of river water, while groundwater in oasis area was greater than that in the mountainous areas, while the concentration of HCO₃⁻, Ca²⁺, K⁺, and Mg²⁺ for river water samples of the lakeside area were higher than that of groundwater (Figure 3).

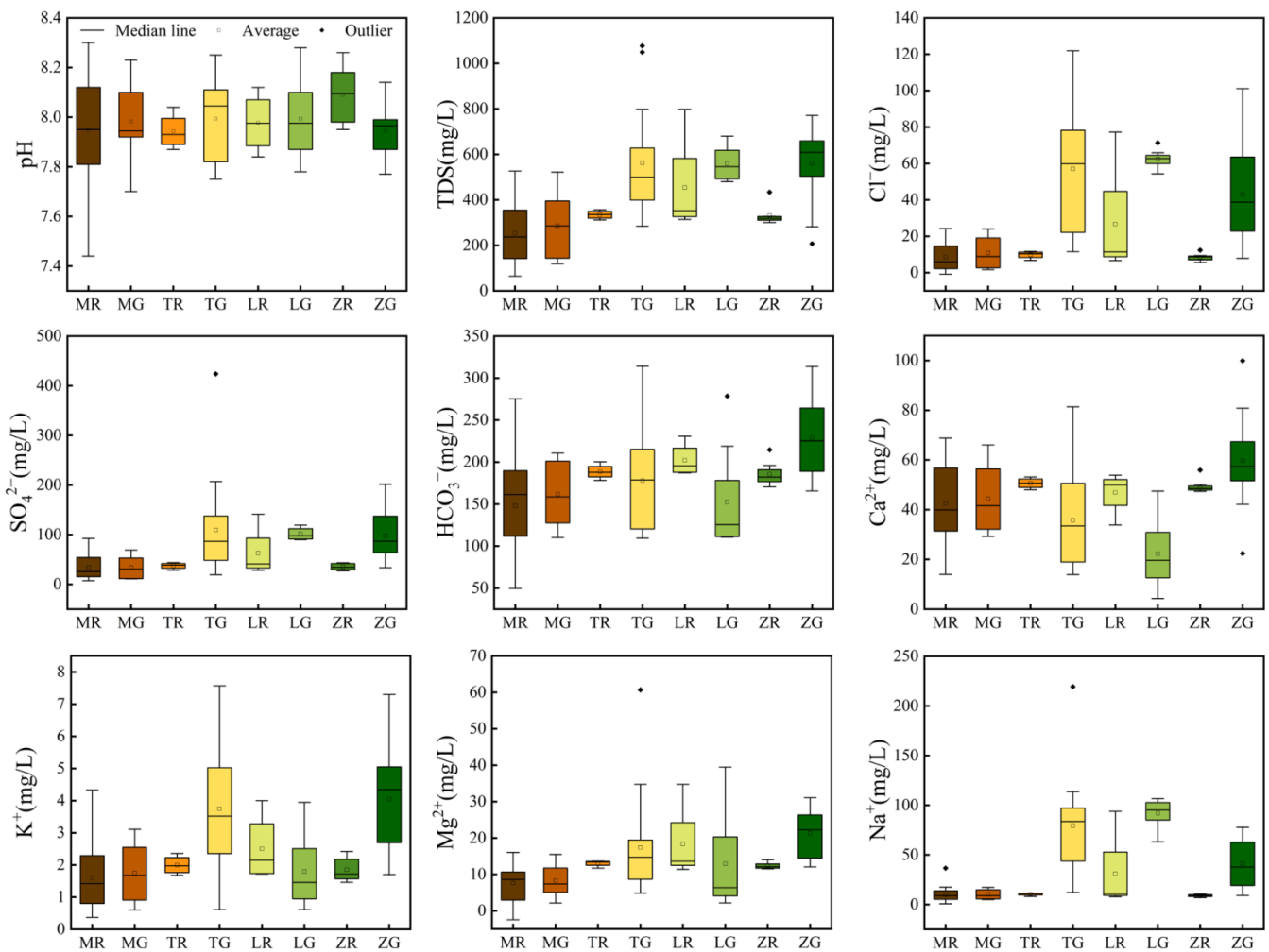


Figure 3. Box diagram of pH, TDS and main ions concentration in different water bodies in mountainous and oasis areas (MR: river water of mountain area, MG: groundwater of mountain area; TR: river water of Traditional oasis area, TG: groundwater of Traditional oasis area; LR: river water of lakeside area, LG: groundwater of Lakeside area; ZR: river water of Transition zone, ZG: groundwater of Transition zone.).

Generally speaking, the ion concentration of groundwater was generally higher than that of river water, and the ion variability of water samples in the mountain regions was relatively smaller than that of the oasis regions.

3.2. Seasonal and Spatial Variations of Stable Isotope

3.2.1. δD and $\delta^{18}O$ in River Water

In this study, river water δD ranged from -99.36 to -61.44% , with an average of -70.39% , and $\delta^{18}O$ ranged from -15.06 to -9.15% , with an average of -10.70% (Table 3). The fluctuation of $\delta^{18}O$ and δD in spring was relatively larger than that in winter, which may be related to the replenishment process of river water by snowmelt water with rich isotopes in spring. On the whole, $\delta^{18}O$ and δD of river water presented an obvious seasonal variation, which was more negative in summer and enrichment in spring. In spring, dryness, less precipitation and vigorous evaporation led to the enrichment of stable isotopes in the river water. In summer, more precipitation and a large amount of ice melt water (with low isotopes) recharged to river water, which resulted in the dilution of stable isotopes in river water samples [4,17,26].

Table 3. δD and $\delta^{18}O$ of surface and groundwater in different seasons.

		Spring			Summer			Autumn			Winter		
		Max	Min	Ave	Max	Min	Ave	Max	Min	Ave	Max	Min	Ave
δD (‰)	groundwater	−59.60	−94.24	−69.12	−53.69	−94.05	−68.55	−51.29	−69.63	−63.86	−60.23	−75.81	−68.31
	river water	−61.44	−99.36	−79.49	−58.35	−71.06	−63.97	−57.52	−73.24	−66.76	−61.41	−76.14	−70.69
	precipitation	−38.47	−76.00	−60.95	6.22	−56.9	−24.15	−13.79	−61.32	−40.13			
	glacier water	−70.05	−153.40	−111.72	−60.19	−67.34	−63.11	−66.34	−70.2	−67.96			
$\delta^{18}O$ (‰)	groundwater	−9.01	−13.86	−10.43	−7.85	−13.54	−10.33	−7.5	−10.75	−9.74	−9.53	−11.7	−10.38
	river water	−9.15	−15.06	−11.62	−9.34	−11.01	−10	−9.39	−10.82	−10.35	−9.52	−11.75	−10.75
	precipitation	−6.02	−11.12	−8.74	0.24	−9.49	−3.94	−2.7	−9.13	−6.74			
	glacier water	−9.97	−20.31	−15.14	−9.65	−10.57	−10.04	−10.33	−10.8	−10.5			

The stable isotope composition of river water samples in the study area showed an obvious spatial variation (Figure 4). The stable isotope of river water in the mountainous area was lower than that in the oasis area, while the stable isotope of river water in the traditional oasis area was higher than that in other areas. The relatively high temperature and the strong evaporation potential in the oasis area may be the main reasons for the relatively high enrichment of stable isotopes in the regional river water. In spring, the $\delta^{18}O$ values of river water showed an order was the traditional oasis area > the transition zone > the lakeside area > the mountain area. In summer, the increasing order of river $\delta^{18}O$ was the traditional oasis area > the lakeside area > the transition zone > the mountains area. In autumn, this trend was the transition zone > the mountain area > the traditional oasis area > the lakeside area. However, the spatial distribution of stable isotopes in river water in winter was similar to spring.

3.2.2. δD and $\delta^{18}O$ in Groundwater

Groundwater samples δD ranged from -51.29 to -94.24 ‰, with an average of -67.29 ‰. Groundwater $\delta^{18}O$ ranged from -7.85 to -13.86 ‰, with an average of -10.19 ‰. The seasonal variation of stable isotopes of groundwater was opposite to that of river water. It is relatively depleted in winter and spring and enriched in autumn. The range of groundwater $\delta^{18}O$ and δD indicated that the groundwater in the study area is significantly affected by surface water in summer, while relatively consistent stable isotope values indicated that the transformation of surface water and groundwater was weaker in winter.

As with the river water, the stable isotopes of groundwater in the study area also presented obviously spatial inconsistency. The stable isotopes of groundwater in the mountainous areas were relatively lower than those in other areas, except in winter. $\delta^{18}O$ and δD values in the lakeside areas was relatively higher, especially in autumn (Figure 4). In spring and summer, groundwater $\delta^{18}O$ values showed a trend of the transition zone > the traditional oasis zone > the lakeside zone > the mountainous area. In autumn, this order was the lakeside zone > the mountainous area > the traditional oasis zone > the transition zone. The spatial variation of groundwater $\delta^{18}O$ in winter was opposite to that in other seasons, which was the mountainous area > the transition zone > the lakeside zone > the traditional oasis zone. The variation of δD value was basically consistent with that of $\delta^{18}O$.

3.2.3. δD and $\delta^{18}O$ in Precipitation and Glacial Water

Precipitation samples δD ranged from -76.00 to 6.22 ‰, with an average of -41.74 ‰, and $\delta^{18}O$ ranged from -11.12 to 0.24 ‰, with an average was -6.47 ‰. The average δD and $\delta^{18}O$ values of precipitation samples were ranked in descending order: summer > autumn > spring. As for glacier water, δD of glacier water samples ranged from -153.40 to -60.19 ‰ with an average of -80.93 ‰, and $\delta^{18}O$ ranged from -120.31 to -9.65 ‰ with an average was -11.89 ‰. The mean δD and $\delta^{18}O$ values descending order of glacier water samples were consistent with precipitation.

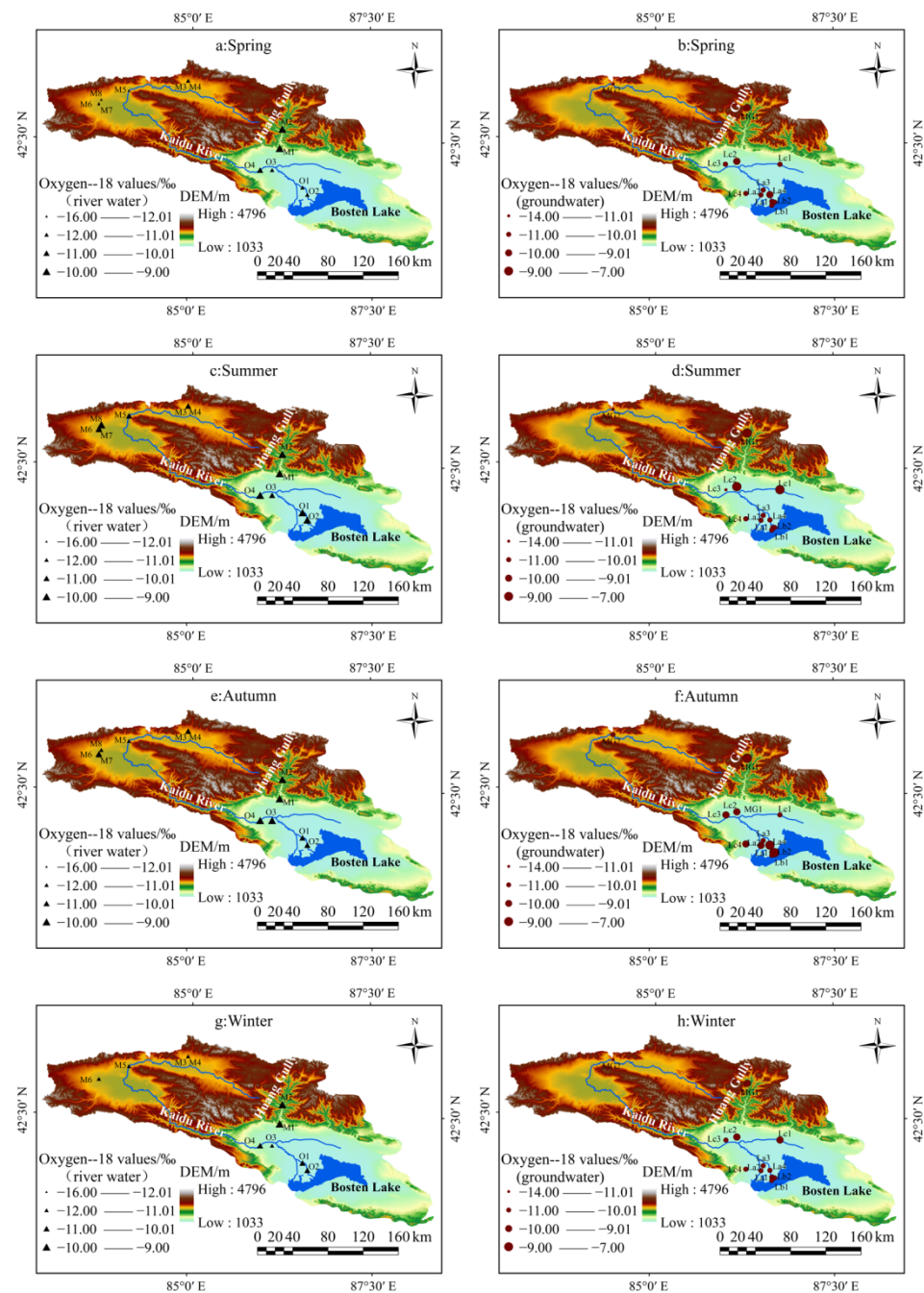


Figure 4. Temporal and spatial distribution characteristics of river water and groundwater $\delta^{18}\text{O}$ in different seasons in the study area. (a) river water $\delta^{18}\text{O}$ in spring; (b) groundwater $\delta^{18}\text{O}$ in spring; (c) river water $\delta^{18}\text{O}$ in summer; (d) groundwater $\delta^{18}\text{O}$ in summer; (e) river water $\delta^{18}\text{O}$ in autumn; (f) groundwater $\delta^{18}\text{O}$ in autumn; (g) river water $\delta^{18}\text{O}$ in winter; (h) groundwater $\delta^{18}\text{O}$ in winter.

3.3. Hydrochemical Types in Surface Water and Groundwater

Hydrochemical types of various water bodies in study area belonged to the $\text{HCO}_3^- \text{Ca}^{2+}$ type (Figure 5). Hydrochemical type of river water was relatively simple, except for river water of the mountain regions in spring. As Figure 4 shown, river water samples collected from the mountain region during spring most located in Ca^{2+} terminal element in the cation diagram, and distributed along the $\text{HCO}_3^- \text{SO}_4^{2-}$ line in the anion diagram, mainly concentrated in the HCO_3^- terminal element. Therefore, the hydrochemical type of the mountain river water in spring can be identified as the $\text{HCO}_3^- \text{SO}_4^{2-} \text{Ca}^{2+}$ type.

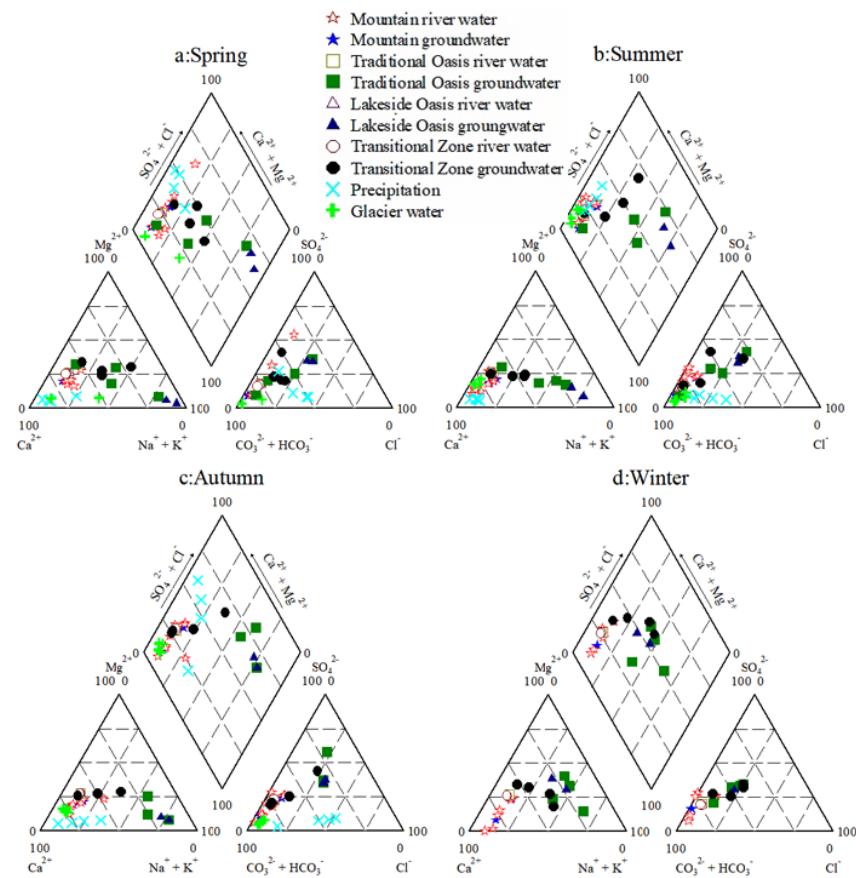


Figure 5. Piper of water bodies in different seasons in the study area. (a) Piper of water bodies in spring; (b) Piper of water bodies in summer; (c) Piper of water bodies in autumn; (d) Piper of water bodies in winter.

Unlike river water, the hydrochemical types of groundwater in the study area presented more complex. The groundwater in the mountainous areas showed the $\text{HCO}_3^- \text{Ca}^{2+}$ type, while the hydrochemical type of groundwater in the oasis area showed obviously seasonal fluctuation. The fluctuating of hydrochemical types of groundwater in the oasis area indicated that groundwater in the oasis area was more sensitive to the influence by external environment than that in the mountainous area.

In the traditional oasis area, the cation map of groundwater was distributed along the $\text{Ca}^{2+}\text{-Na}^+$ line in spring and summer, and the anion was concentrated at the end of HCO_3^- terminal. The hydrochemical type in this period was defined as the $\text{HCO}_3^- \text{Ca}^{2+}\text{-Na}^+$ type. In autumn, cations gathered at the $\text{Na}^+ + \text{K}^+$ terminal, anions were located in the $\text{HCO}_3^- \text{Cl}^-$ line and tended to SO_4^{2-} terminal, which belonged to the $\text{SO}_4^{2-}\text{-Cl}^- \text{Na}^+$ type. In winter, anions were more dropped into HCO_3^- terminal element, and hydrochemical type belonged to the $\text{HCO}_3^- \text{Ca}^{2+}\text{-Na}^+$ type. In the lakeside area, the cation of water samples in spring, summer and autumn were located in the terminal element of $\text{Na}^+ + \text{K}^+$, the anions were in the middle and lower position, and the hydrochemical type belonged to $\text{HCO}_3^- \text{Cl}^- \text{Na}^+$ type. In winter, the cations fell in the middle and lower position, and most anions located in the terminal element of HCO_3^- , which indicated the hydrochemical type was the $\text{HCO}_3^- \text{Na}^+ \text{Mg}^{2+}$ type. In the transition zone, the groundwater hydrochemical type belonged to the $\text{HCO}_3^- \text{SO}_4^{2-} \text{Ca}^{2+} \text{Na}^+$ type. The hydrochemical types of precipitation and glacier water were similar, both of which belonged to $\text{HCO}_3^- \text{Ca}^{2+}$ type.

4. Discussion

4.1. Factors Controlling Hydrochemical Processes

Gibbs diagram is an important method to determine the source of the main chemical components in natural water. It can clearly point out the impact of precipitation control, rock weathering and evaporation concentration on the hydrochemical process [45,46]. As shown in Figure 6, most of water samples fell in the low value area of $\text{Cl}^- / (\text{Cl}^- + \text{HCO}_3^-)$ in the Gibbs diagram, while the TDS value was distributed between 100 and 1100 mg/L, indicating that hydrochemical composition of most water bodies in the study area were mainly controlled by rock weathering. It is worth noting that some groundwater samples of the oasis areas fell outside the three typical control areas. In the Gibbs diagram, the ratio of $\text{Na}^+ / (\text{Na}^+ + \text{Ca}^{2+})$ of these samples were greater than 0.5. Previous studies [36–38] suggested that this phenomenon was caused by the interference of human activities. Irrigated agriculture was widely distributed in oasis region of the study area, which had an obvious influence on the regional groundwater environment. In the area of human disturbance of Gibbs diagram, groundwater samples in the oasis area and lakeside area were obvious more than those in the transition zone, which indicated that the groundwater environment in the traditional oasis area and lakeside area were more obviously disturbed by human activities.

4.2. Relationship between Surface Water and Groundwater

As an important part of hydrological system, the interaction between surface water and groundwater has been observed in various topographical and climatic landscapes. In order to manage water resources, it is necessary to understand the interaction between groundwater and surface water. The study area is not only an important oasis agricultural area in Xinjiang, but also a concentrated area of population and cities. The large-scale development of agricultural activities and the increase of domestic water demand leads to the complex relationship between surface water and groundwater in the study area. EMMA (end member mixing analysis) method is a widely used hydrological segmentation method, which has been applied to study the relationship between different water bodies.

According to the EMMA method (Figure 7), this study explores the relationship between surface water and groundwater in the study area, based on TDS and $\delta^{18}\text{O}$ values of groundwater and surface water samples (river water and precipitation and snow melt water) during difference seasons. In a word, most groundwater samples were located in the triangle area composed of precipitation, river water and previous groundwater samples, which indicated that there was an obvious relationship between surface water and groundwater in this area (river water and precipitation and snow melt water).

In spring, there was a small number of river water samples in mountainous areas plotted in the triangle composed of the average values of tracer TDS and $\delta^{18}\text{O}$ of groundwater, river water and precipitation, which indicated that significant transformation relationship between the groundwater and surface water (precipitation and river water). In summer, most of the river water in mountainous areas fell into the triangle area composed of groundwater, snow melt water and precipitation, which indicated the river water recharged by groundwater, snow melt water and precipitation in this period. However, groundwater in mountainous areas was far away from surface water samples, which suggested the interaction between groundwater and surface water (river water, precipitation and snow melt water) was not obvious in summer. In autumn, most of river water and groundwater samples in mountainous areas were located in the triangular region, indicated that the interaction between surface water and groundwater was obvious.

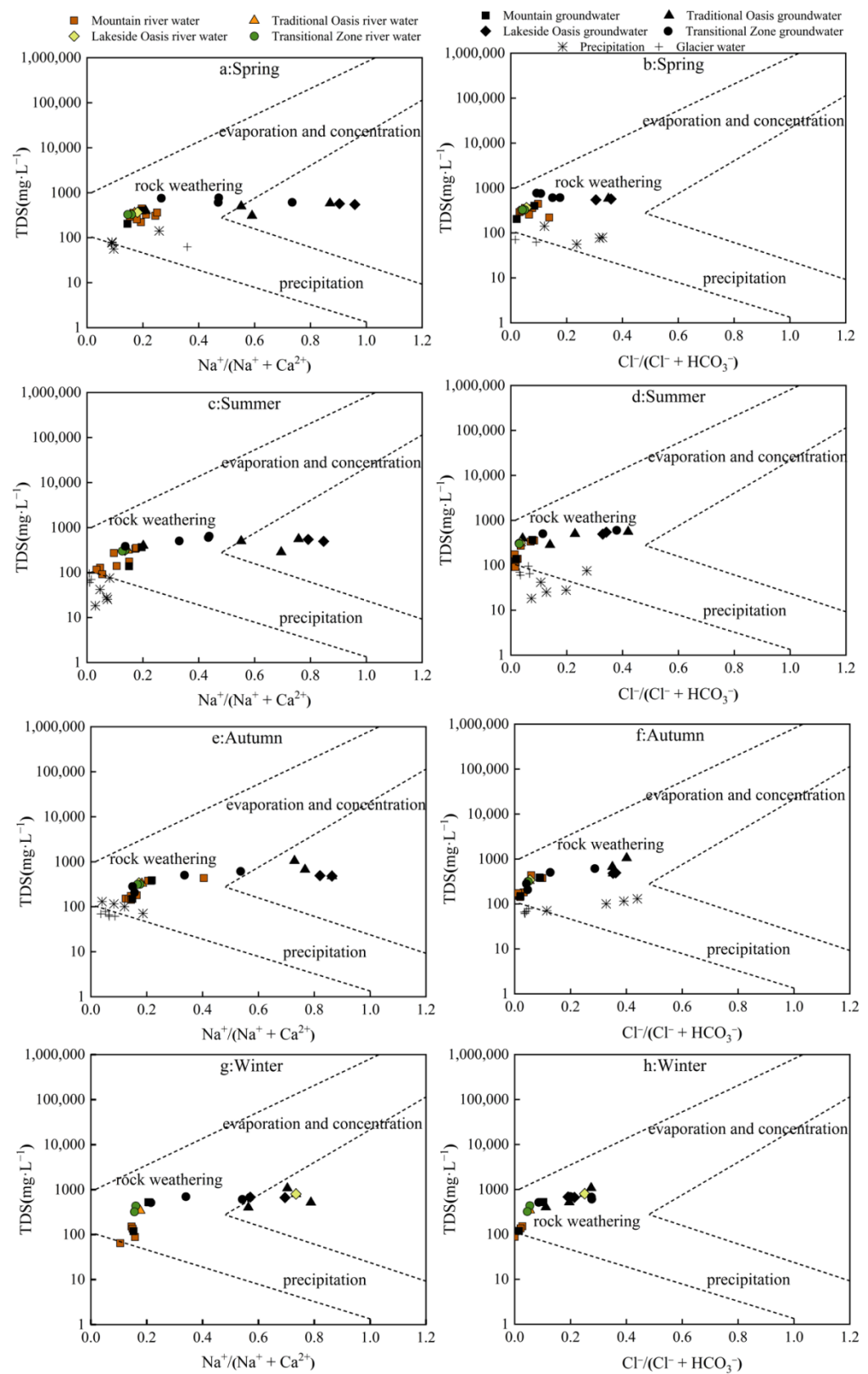


Figure 6. Gibbs of water bodies in different seasons in the study area. (a) Gibbs of water bodies in spring; (b) Gibbs of water bodies in spring; (c) Gibbs of water bodies in summer; (d) Gibbs of water bodies in summer; (e) Gibbs of water bodies in autumn; (f) Gibbs of water bodies in autumn; (g) Gibbs of water bodies in winter; (h) Gibbs of water bodies in winter.

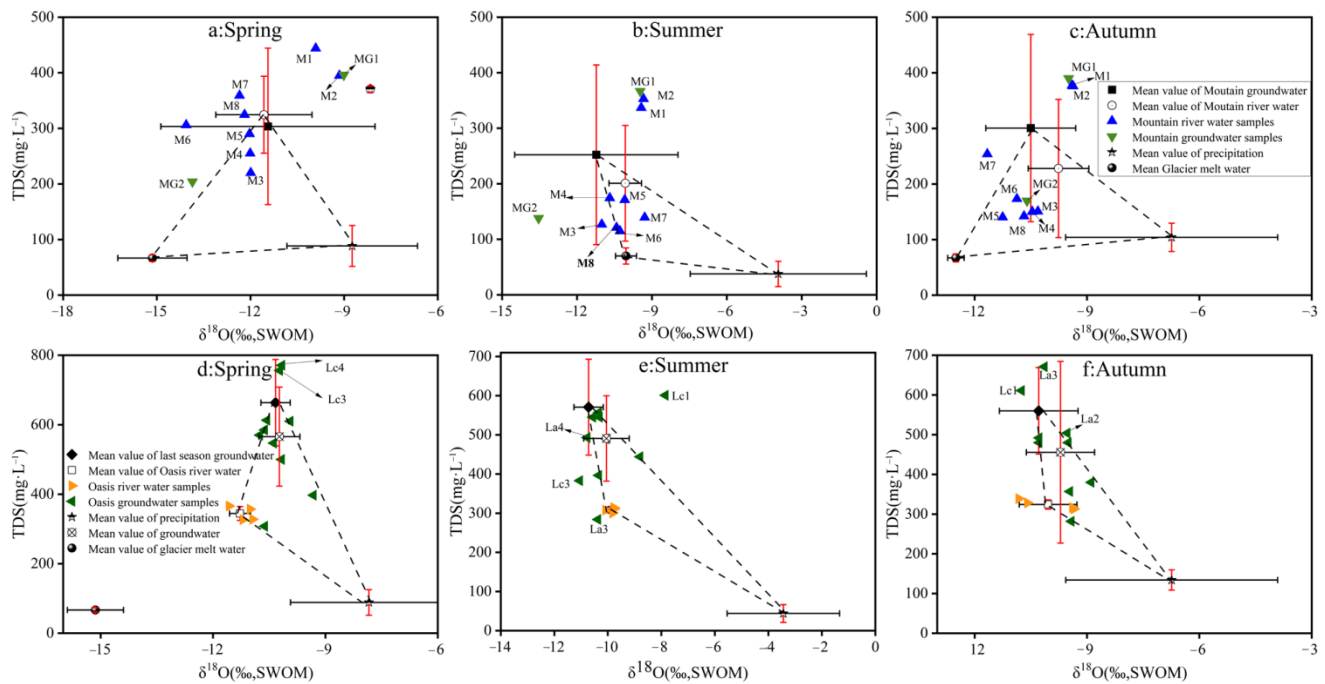


Figure 7. The EMMA map between surface water and groundwater based on the tracers of TDS and $\delta^{18}\text{O}$ in the study area. (a) the EMMA map in mountain in spring; (b) the EMMA map in mountain in summer; (c) the EMMA map in mountain in autumn; (d) the EMMA map in oasis in spring; (e) the EMMA map in oasis in summer; (f) the EMMA map in oasis in autumn.

In the oasis area, the river water and groundwater samples fell into the triangular field composed of three ends (precipitation, groundwater and river water) during spring, indicated that groundwater was a mixture of three streamflow composition. In summer, most of the groundwater and river water samples in the oasis area located at the periphery and edge of the triangle area composed of groundwater, river water, and precipitation, indicated that the relationship between surface water and groundwater was weak in this period. In autumn, rivers and groundwater in mountainous and oasis areas dropped in the middle of the triangular region (groundwater, ice melt water and precipitation), indicated an obvious transformation relationship between surface water and groundwater were observed in this period.

According to three-component method, the ratios of interaction between groundwater and various recharging water sources was calculated. Figure 8 indicated the groundwater in the oasis area was mainly controlled by groundwater in the previous season. In addition, river water and precipitation also occupied a certain supply proportion, and the contribution of river water to groundwater was greater than precipitation. The hydraulic connections between groundwater and surface water also presented obvious seasonal inconsistencies. In spring, groundwater in the lakeside area and the traditional oasis area was significantly affected by the river water. In the spring, the large-scale development of groundwater caused by agricultural drought and water shortage for agricultural irrigation often leads to the decline of shallow groundwater, further leading to more river water contributed regional groundwater. In summer, groundwater in the transition zone was more significantly affected by precipitation, while precipitation had weak influence on groundwater in the traditional oasis area. In autumn, the contribution of precipitation in traditional oasis areas on groundwater (the contribution rate was 16.4%) was greater than that of river water. In the traditional oasis area, the interaction between river water and groundwater is more obviously, especially in spring and summer, which require governor to pay more attention to regional water environment of river water in this area and reduce

the risk of river water pollution, and avoid the deterioration of groundwater environment caused by the river water replenishing groundwater.

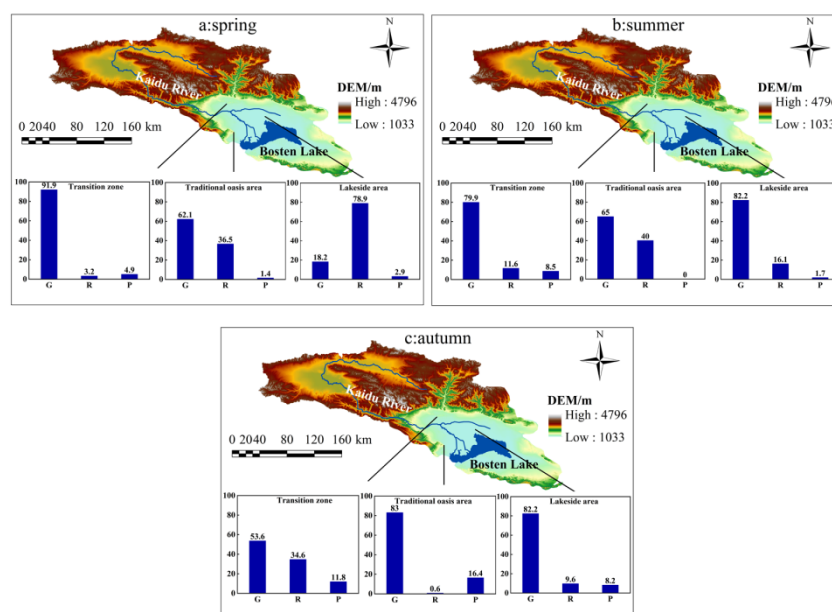


Figure 8. Recharge ratio of surface water and groundwater in the oasis area during different seasons (G: groundwater in previous season, R: river water, P: precipitation). (a) Recharge ratio of surface water and groundwater in the oasis area in spring; (b) Recharge ratio of surface water and groundwater in the oasis area in summer; (c) Recharge ratio of surface water and groundwater in the oasis area in autumn.

4.3. Ion Ratio of Dissolved Minerals and Cation Exchange

The ionic ratios can reflect the dissolution of different minerals produces different types or ratios of ions, and further help analyze the effects of the dissolution of different minerals on groundwater chemistry [47]. In order to further explore the ionic ratios of dissolved minerals, this study mapped the Scatter plots of major ions (Figure 9). All surface water and groundwater were further divided on the basis of the plots of $(Ca^{2+} + Mg^{2+})$ versus $(Na^{+} + K^{+})$. As Figure 9a shown surface water samples of this study were mainly controlled by the dissolution of silicate and carbonate, with precipitation and glacial water being affected more strongly. Groundwater samples were mainly affected by evaporation, while a few groundwater samples in the transition zone and the mountainous areas were controlled by the dissolution of carbonate (Figure 9b). The silicate weathering or a cation exchange can reflected by the Na^{+}/Cl^{-} ratio [45,47].

As shown in Figure 9c,d, Na^{+} and Cl^{-} equivalent concentrations in surface water samples and some groundwater samples were mostly lower than 5 meq/L and generally near the 1:1 line, mainly controlled by the rock salt dissolution, but the Cl^{-} equivalent concentration of river water in the transition zone was high, corresponding to the chlorine hydrochemical type in the transition zone. In some samples of the traditional oasis and lakeside areas, the concentration of Na^{+} was significantly higher than the Cl^{-} concentration, mainly attributable to Na^{+} overflow, there should also be other anions to balance the excess sodium ions, this indicates that Na^{+} has other major sources apart from rock weathering. Silicate weathering, anthropogenic input, and ion exchange may contribute to the redundant Na^{+} [48].

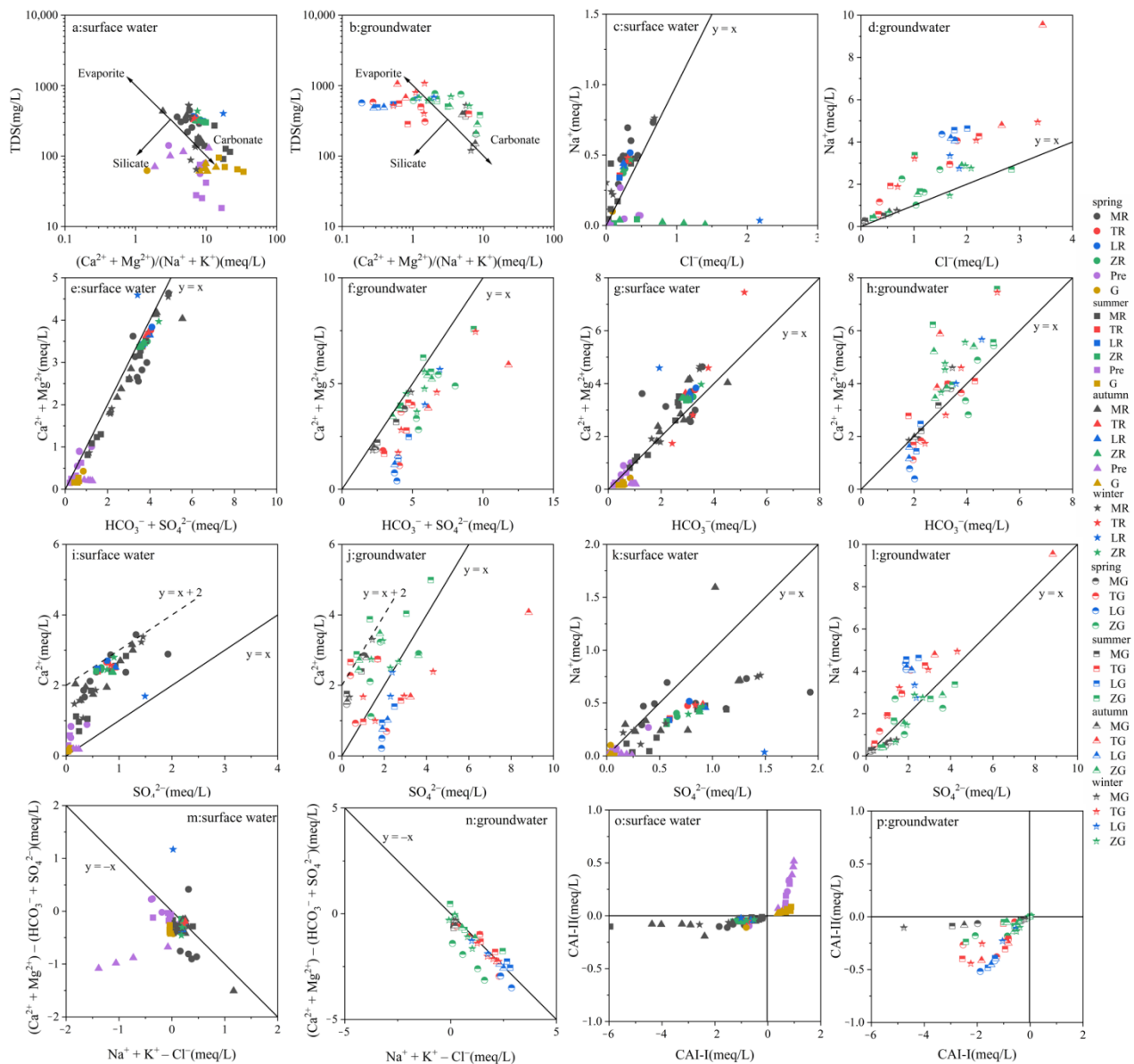


Figure 9. Scatter plots of major ions. (a) $(Ca^{2+} + Mg^{2+})$ versus $(Na^{+} + K^{+})$ in surface water, (b) $(Ca^{2+} + Mg^{2+})$ versus $(Na^{+} + K^{+})$ in groundwater; (c) Na^{+} versus Cl^{-} in surface water, (d) Na^{+} versus Cl^{-} in groundwater; (e) $(Ca^{2+} + Mg^{2+})$ versus $(HCO_3^{-} + SO_4^{2-})$ in surface water, (f) $(Ca^{2+} + Mg^{2+})$ versus $(HCO_3^{-} + SO_4^{2-})$ in groundwater; (g) $(Ca^{2+} + Mg^{2+})$ versus HCO_3^{-} in surface water, (h) $(Ca^{2+} + Mg^{2+})$ versus HCO_3^{-} in groundwater; (i) Ca^{2+} versus SO_4^{2-} in surface water, (j) Ca^{2+} versus SO_4^{2-} in groundwater; (k) Na^{+} versus SO_4^{2-} in surface water, (l) Na^{+} versus SO_4^{2-} in groundwater; (m) $[(Ca^{2+} + Mg^{2+}) - (HCO_3^{-} + SO_4^{2-})]$ versus $(Na^{+} + K^{+} - Cl^{-})$ in surface water, (n) $[(Ca^{2+} + Mg^{2+}) - (HCO_3^{-} + SO_4^{2-})]$ versus $(Na^{+} + K^{+} - Cl^{-})$ in groundwater; (o) CAI-I versus CAI-II in surface water, (p) CAI-I versus CAI-II in groundwater. (MR: river water of Mountain area, MG: groundwater of Mountain area; TR: river water of Traditional oasis area, TG: groundwater of Traditional oasis area; LR: river water of Lakeside area, LG: groundwater of Lakeside area; ZR: river water of Transition zone, ZG: groundwater of Transition zone, Pre: precipitation, G: glacier).

The ratio of $(Ca^{2+} + Mg^{2+})/(HCO_3^{-} + SO_4^{2-})$ can reflect the calcite weathering. If the water sample hydrochemistry is mainly controlled by the dissolution of calcite ($CaCO_3$), dolomite ($CaMg(CO_3)_2$), and gypsum or anhydrite ($CaSO_4$), then $(Ca^{2+} + Mg^{2+})$ and $(HCO_3^{-} + SO_4^{2-})$ should be distributed near the 1:1 line [49]. The equivalent concentration ratio of $(HCO_3^{-} + SO_4^{2-})/(Ca^{2+} + Mg^{2+})$ in the water samples in the study area were

around the 1:1 line (Figure 9e,f). To further clarify the type of dissolved carbonate rock, the $(\text{Ca}^{2+} + \text{Mg}^{2+})$ and HCO_3^- plot was generated, as shown in Figure 9g,h.

The $(\text{Ca}^{2+} + \text{Mg}^{2+})$ and HCO_3^- plot was displayed in Figure 9g,h, a large number of water samples were distributed around the $y = x$ line, which shows that the geochemical composition of water samples is mainly controlled by the dissolution of calcite or dolomite [46,50].

In naturally, Ca^{2+} and SO_4^{2-} were derived from weathering of gypsum, the molar ratio of $\text{Ca}^{2+}/\text{SO}_4^{2-}$ usually be 1:1 [51]. Figure 9i,j showed the relation between Ca^{2+} and SO_4^{2-} . It was observed that most of river water samples and groundwater samples were mainly distributed close to the $y = x + 2$ line. While the groundwater samples of the lakeside area were mostly located near the $y = x$ line, which indicated groundwater of the lakeside area was mainly affected by the dissolution of gypsum. The sources of Na^+ and SO_4^{2-} in samples could be inferred from the $\text{Na}^+/\text{SO}_4^{2-}$ plot in Figure 9k,l. Sample distribution along the $y = x$ line was symmetrical, but still varies significantly [47]. In particular, SO_4^{2-} equivalent concentrations of some river water was higher than that of Na^+ , thus Na^+ and SO_4^{2-} may be strongly affected by human activities [10].

Cation exchange is a common chemical reaction between groundwater and water-bearing rock formations [52]. When cation exchange occurs forward Na^+ and K^+ in groundwater replace Ca^{2+} and Mg^{2+} in minerals [53]. The scatter plot between the ionic charge of $[(\text{Ca}^{2+} + \text{Mg}^{2+}) - (\text{HCO}_3^- + \text{SO}_4^{2-})]$ and $(\text{Na}^+ + \text{K}^+ - \text{Cl}^-)$ was used to verify whether cation exchange had a significant effect on the chemical composition of groundwater. This conjecture is verified when its ratio is approximately -1 . As shown in Figure 9m,n, all water samples in the study area were located around the $-1:1$ line, indicating that cation exchange has a significant effect on the development of river water and groundwater chemical composition in the study area.

The chlor-alkali index (CAI) can further indicate the direction along which cation exchange occurs, with two indicators: CAI-I for $(\text{Cl}^- - \text{Na}^+ - \text{K}^+)/\text{Cl}^-$ and CAI-II for $(\text{Cl}^- - \text{Na}^+ - \text{K}^+)/(\text{HCO}_3^- + \text{SO}_4^{2-} + \text{Cl}^- + \text{NO}_3^-)$. When $\text{CAI} > 0$, the cation exchange action is forward; when $\text{CAI} < 0$, the cation exchange action is reverse [54]. As shown in Figure 9o,p, $\text{CAI} < 0$ for most samples in groundwater and river water, $\text{Ca}^{2+} + \text{Mg}^{2+}$ in water replaced Na^+ and K^+ in minerals.

4.4. Effects of Human Activities

In this study, some of the ions such as SO_4^{2-} , Ca^{2+} , and Na^+ showed characteristics clearly beyond the control of natural causes, which indicated a strongly influence of human activities on regional groundwater samples. In contrast to natural causes, human activities release agricultural fertilizers, industrial wastewater, and domestic sewage into groundwater, resulting in the input of large amounts of SO_4^{2-} , Cl^- , and NO_3^- [55]. Among naturally produced ions, NO_3^- is generally produced in small amounts by nitrification, and several studies have shown that higher concentrations of NO_3^- in groundwater are generally associated with agricultural activities [55]. The end-element diagram of $(\text{NO}_3^-/\text{Na}^+)$ and $(\text{Cl}^-/\text{Na}^+)$ is used to analysis the impact of agricultural activities on river water and groundwater (Figure 10a,b). As a whole, agricultural activities have relatively stronger influence on the river water in the oasis area, especially in the transition zone and the lakeside area. However, the influence of agricultural activities on the lakeside area river water was more obviously than in other areas especially in winter. The groundwater in the oasis area was also obviously affected by human activities, especially in the transition zone and the lakeside area. The strong influence of agricultural activities on the transition zone groundwater is greatly influenced by agricultural activities is closely related to the geological environment of the area. The transition zone is located at the junction of the mountain and oasis areas and regional soil is dominated by gravel, with large porosity and strong infiltration, so human activities (such as farming and fertilization) can easily cause the variation of groundwater environment. The lakeside area is located in the junction region of the Kaidu river and the Bosten lake and the interaction between river water,

groundwater and lake water was more frequently. Naturally, NO_3^- and other elements from surface tillage to migrate to the groundwater system [56]. In this study, long history of farming of the traditional oasis area caused the cultivation layer is thick and the soil gap is small, the groundwater is buried deep and the surface water seeps slowly. Therefore, the interaction between surface water and groundwater in this region was weak and the influence of human activities on the traditional oasis region was relatively weak. In addition, the groundwater in the oasis area is also affected by the evaporation especially in the summer.

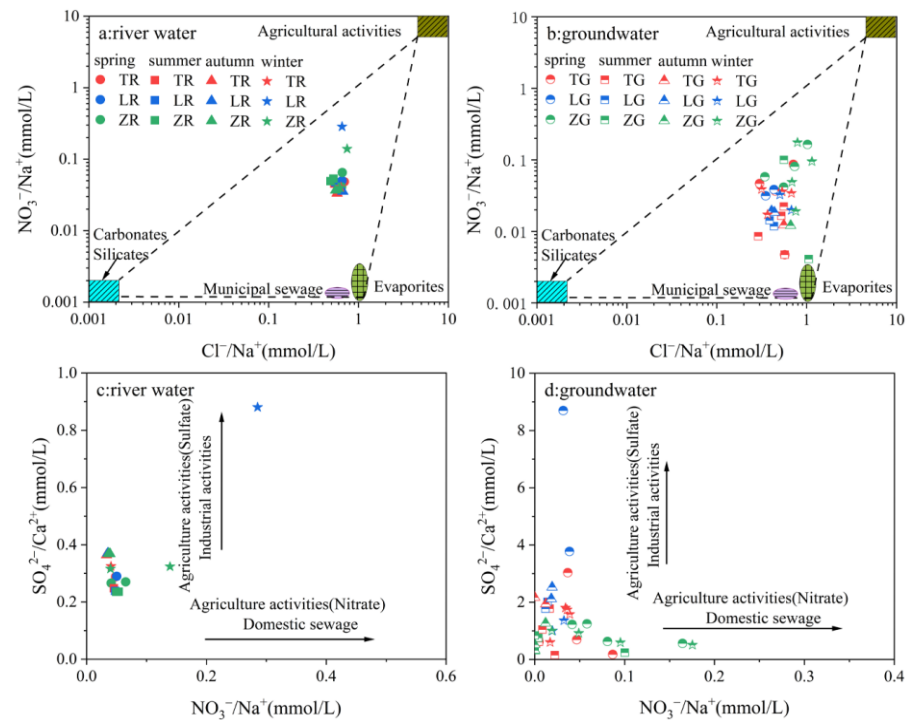


Figure 10. Plots of (a) Cl^-/Na^+ versus $\text{NO}_3^-/\text{Na}^+$ in river water, (b) Cl^-/Na^+ versus $\text{NO}_3^-/\text{Na}^+$ in groundwater; (c) $\text{NO}_3^-/\text{Na}^+$ versus $\text{SO}_4^{2-}/\text{Ca}^{2+}$ in river water, (d) $\text{NO}_3^-/\text{Na}^+$ versus $\text{SO}_4^{2-}/\text{Ca}^{2+}$ in groundwater. (TR: river water of Traditional oasis area, LR: river water of Lakeside area, ZR: river water of Transition zone; TG: groundwater of Traditional oasis area; LG: groundwater of Lakeside area; ZG: groundwater of Transition zone).

In this study, the ratio diagram of ($\text{SO}_4^{2-}/\text{Ca}^{2+}$) and ($\text{NO}_3^-/\text{Na}^+$) was adopted to comprehensively represent the pollution of groundwater by two major types of pollution, sulfur-containing fertilizers and industrial wastewater and nitrate-containing fertilizers and domestic wastewater [56]. Results shown river water and groundwater of the oasis region were mainly contaminated by sulphate-containing fertilizers and industrial wastewater (Figure 10c,d).

4.5. Differences from the Other Regions

In order to further analyze the heterogeneity of hydrochemistry distribution in the inland arid areas of China, the Hexi Corridor (including Shiyang river basin, Heihe river basin and Shule river basin), Tarim Basin and the inland river basins on the northern slope of Tianshan Mountain (Urumqi river basin and Yili river basin) were selected as compare region to reveal difference of main hydrochemistry factors and influencing factors in these regions [57].

In general, the river water in the inland area of northwest China was slightly alkaline, and its pH value was between 7 and 10. The TDS value of river water was generally higher (between 19 to 30,000 $\text{mg}\cdot\text{L}^{-1}$). Compared with other regions in China, the hydrochemical

types mainly belonged to $\text{Na}^+\text{-SO}_4^{2-}$, $\text{Mg}^{2+}\text{-SO}_4^{2-}$ and $\text{Ca}^{2+}\text{-HCO}_3^-$ type. Table 4 suggested obviously spatial inconsistencies for hydrochemical compositions were observed in the Northwest China. The pH value of river water in the Tarim basin was generally higher than that in other regions, while the pH value of river water in the Urumqi river basin on the north slope of Tianshan Mountain fluctuates greatly, and the pH value of inland river in the Hexi Corridor was relatively smaller. Comparing with three regions, it is found that the main ions in inland river water of the northwest China were Ca^{2+} , Na^+ , Mg^{2+} , HCO_3^- and SO_4^{2-} . The river water chemical types of the Hexi Corridor and the Tarim Basin were similar to $\text{Na}^+\text{-SO}_4^{2-}$ and $\text{Mg}^{2+}\text{-SO}_4^{2-}$ type, while the Urumqi river basin was completely inconsistent with other regions, which was $\text{Ca}^{2+}\text{-HCO}_3^-$ type.

Compared with surface river water, the groundwater environment in the arid inland area of Northwest China was more complex. The pH value of groundwater was similar to that of river water, which was weakly alkaline. However, pH value of groundwater in inland river of the north slope of Tianshan Mountain and Tarim River Basin were significantly higher than that of river water, which may be related to the more extreme arid environment. The TDS value of groundwater of the northwest China presented a larger range, with 20 to 30,000 $\text{mg}\cdot\text{L}^{-1}$. In the northwest arid area, the hydrochemical type of groundwater in most inland river basin belonged to $\text{Ca}^{2+}\text{-HCO}_3^-$ type, except for the Hexi corridor region, which was generally $\text{Mg}^{2+}\text{-SO}_4^{2-}$, $\text{Ca}^{2+}\text{-Mg}^{2+}\text{-HCO}_3^-$ - SO_4^{2-} , or $\text{Na}^+\text{-Mg}^{2+}\text{-SO}_4^{2-}\text{-Cl}^-$ type. The $\delta^{18}\text{O}$ and δD values of surface water and groundwater showed significant spatial inconsistency in the northwest regions, of which surface water stable isotope were generally smaller, with $\delta^{18}\text{O}$ between -30‰ and 4‰ and δD between -250‰ and 5‰ . Although the stable isotope value of river water in Hexi corridor was small and fluctuating, which may be related to the complex streamflow components of inland rivers in this region. The stable isotopes of groundwater in the arid inland area of the northwestern China were generally greater than those of surface water [18,25,58].

As a typical mountain–oasis ecosystem, the study area (combined alpine and oasis climate pattern) is located in the central part of the northwestern arid region and the transition zone [44]. Hydrological circulation process of the study area is not only affected by natural environment, but also controlled by human disturbance to a certain extent. The pH value range of surface water in the study area was similar to that in the Tarim river basin, while the TDS value range of surface water was similar to that of the Hexi corridor region. In this study area, the TDS value of groundwater ranged from 19 to 1077 $\text{mg}\cdot\text{L}^{-1}$, which was lower than that in other regions except for the Urumqi river basin. However, the hydrochemical types of river water in the study area were relatively stable, which were consistent with those in the Urumqi river basin. The hydrochemical types of groundwater were relatively complex. The hydrochemical types of groundwater in mountainous areas were $\text{Ca}^{2+}\text{-HCO}_3^-$ type consistent with those in the whole northwest region. The groundwater in oasis areas presented different hydrochemical types in different seasons, such as HCO_3^- - Ca^{2+} - Na^+ type, SO_4^{2-} - Cl^- - Na^+ type, HCO_3^- - Ca^{2+} - Na^+ type and HCO_3^- - Na^+ - Mg^{2+} type. The hydrochemical process in the study area was controlled by rock weathering and human activities, which was similar to the Urumqi river basin.

Table 4. Differences of hydrochemical characteristics in different regions of Northwestern China.

Location		Surface Water				Groundwater				References
		pH	TDS (mg/L)	$\delta^{18}\text{O}$ (‰)	δD (‰)	pH	TDS (mg/L)	$\delta^{18}\text{O}$ (‰)	δD (‰)	
Hexi corridor region	Shiyang River	7.0~8.4	64~353	−10.0~−1.8	−60.6~−14.5	7.0~8.5	231~20,897	−11.3~−5.0	−86.2~−28.5	[58]
	Heihe River	7.2~8.1	31~2157	−29.7~1.9	−216.3~38.7	7.2~8.1	293~5157	−9.7~−3.7	−58.0~−42.0	[25]
	Shule River	7.2~7.8	19~980	−29.0~3.8	−233.1~36.5	7.6~7.9	117~2382	−11.9~−6.9	−63.1~−9.4	[18,59]
North slope of Tianshan	Urumqi River	6.0~8.5	125~304	−36.2~0.0	−67.5~−44.0	7.0~7.9	128~245	−9.0~−8.9	−61.0~−57.0	[27]
	Yili River	7.2~8.4	303~321	−11.6~−10.9	−77.0~−72.0					[46,60]
Tarim Basin	Tarim River	7.4~8.5	253~3220	−25.74~8.48	−96.1~51.9	7.2~8.8	450~27,495			[9,17,26]
	Yarkant River	7.4~8.3	273~3344			6.4~8.6	522~9014			[61]
Study area		7.4~8.3	64~798	−15.0~−9.2	−99.4~−61.4	7.7~8.3	19~1077	−13.8~−7.8	−94.2~−51.3	

Variation of controlling factors usually results in water environment variability. Compared with the main control factors of water chemistry in different regions, rock weathering and evaporation concentration were the main influencing factors of water environment changes in arid areas of northwest inland [58]. The influence of rock weathering on the Tarim River and the Shule River were obvious. In addition, the inland river basin of northwestern China were affected by different degrees of human activities, especially in the oasis regions [26,61].

5. Conclusions

Most surface water and groundwater was mildly alkaline. HCO_3^- and Na^+ were the main anions and cations for different water body. Hydrochemical distribution had significant seasonal and spatial variation in the study area. The stable isotopes of surface water and groundwater in the study area also presented significant spatial inconsistency. Higher $\delta^{18}\text{O}$ values appeared in most of water samples collected from the oasis area and lower $\delta^{18}\text{O}$ values appeared in the mountain area.

Most of water bodies in the study areas belonged to $\text{HCO}_3^- \text{Ca}^{2+}$ type. The hydrochemical type of groundwater presents obviously spatial inconsistency than that of surface water. $\text{HCO}_3^- \text{Ca}^{2+}$ type mainly observed in groundwater samples of mountainous area, while the groundwater in oasis area showed variability hydrochemical types in different seasons. River water samples were mainly controlled by the dissolution of carbonate, and groundwater samples were mainly affected by evaporation. Agricultural activities had influence on the groundwater environment in the oasis area.

The surface water–groundwater interaction also displays spatial inconsistency in this study, especially in summer. In oasis area, groundwater was mainly controlled by previous season groundwater, river water and precipitation also occupied a certain supply proportion. The hydraulic connections between groundwater and surface water also presented obvious seasonal inconsistencies. The transformation of river water and groundwater in the traditional oasis area is more obvious, so attention should be paid to the water environment of the surface river water in this area to avoid the polluted river water affecting the regional groundwater system.

Author Contributions: Conceptualization, C.S. and S.W.; methodology, C.S.; software, S.W.; validation, C.S., W.C. and S.W.; formal analysis, W.C.; investigation, S.W.; resources, C.S.; data curation, W.C.; writing—original draft preparation, S.W.; writing—review and editing, C.S. and S.W.; visualization, S.W.; supervision, W.C.; project administration, C.S.; funding acquisition, C.S. All authors have read and agreed to the published version of the manuscript.

Funding: This research was supported by the National Natural Science Foundation of China [Grant No. 41901022] and the China desert Meteorological Science Research Foundation [Grant No. Sqj2021020].

Data Availability Statement: Not applicable.

Conflicts of Interest: The authors declare no conflict of interest.

References

1. Panneerselvam, B.; Paramasivam, S.K.; Karuppanan, S.; Ravichndran, N.; Selvaraj, P. A GIS-based evaluation of hydrochemical characterisation of groundwater in hard rock region, South Tamil Nadu, India. *Arab. J. Geosci.* **2020**, *13*, 837. [[CrossRef](#)]
2. He, X.; Wu, J.; He, S. Hydrochemical characteristics and quality evaluation of groundwater in terms of health risks in Luohe aquifer in Wuqi County of the Chinese Loess Plateau, northwest China. *HERA Int. J.* **2019**, *25*, 32–51. [[CrossRef](#)]
3. Xu, J.; Chen, Y.; Li, W.; Zhang, L.; Hong, Y.; Bi, X.; Yang, Y. Statistical analysis of groundwater chemistry of the Tarim River lower reaches, Northwest China. *Environ. Earth Sci.* **2012**, *65*, 1807–1820. [[CrossRef](#)]
4. Long, M.; Wu, J.; Abuduwaili, J. Hydrochemical and isotopic characters of surface water in agricultural oases of the Tianshan Mountains, Northwest China. *Arid. Land Res. Manag.* **2016**, *30*, 37–48. [[CrossRef](#)]
5. Alexakis, D.E. Linking DPSIR Model and Water Quality Indices to Achieve Sustainable Development Goals in Groundwater Resources. *Hydrology* **2021**, *8*, 90. [[CrossRef](#)]
6. Masoud, A.A. On the Retrieval of the Water Quality Parameters from Sentinel-3/2 and Landsat-8 OLI in the Nile Delta's Coastal and Inland Waters. *Water* **2022**, *14*, 593. [[CrossRef](#)]

7. Alexakis, D.E. Meta-evaluation of water quality indices. application into groundwater resources. *Water* **2020**, *12*, 1890. [[CrossRef](#)]
8. Sun, C.; Chen, W.; Shen, Y. The seasonal and spatial distribution of hydrochemical characteristics of groundwater and its controlling factors in the eastern Loess Plateau. *Earth Sci. Inform.* **2021**, *14*, 2293–2308. [[CrossRef](#)]
9. Wang, W.; Chen, Y.; Wang, W.; Xia, Z.; Li, X.; Kayumba, P.M. Hydrochemical characteristics and evolution of groundwater in the dried-up river oasis of the Tarim Basin, Central Asia. *J. Arid. Land* **2021**, *13*, 977–994. [[CrossRef](#)]
10. Thomas, J.; Joseph, S.; Thrivikramji, K.P. Hydrochemical variations of a tropical mountain river system in a rain shadow region of the southern Western Ghats, Kerala, India. *Appl. Geochem.* **2015**, *63*, 456–471. [[CrossRef](#)]
11. Ayuba, R.; Tijani, M.N.; Snow, D. Hydrochemistry and stable isotopes (^{18}O and ^2H) characteristics of groundwater in Lokoja and its environs, central Nigeria. *Environ. Earth Sci.* **2019**, *78*, 582. [[CrossRef](#)]
12. Emenike, P.C.; Nnaji, C.C.; Tenebe, I.T. Assessment of geospatial and hydrochemical interactions of groundwater quality, southwestern Nigeria. *Environ. Monit. Assess.* **2018**, *190*, 440. [[CrossRef](#)] [[PubMed](#)]
13. Chukwura, U.O.; Udom, G.J.; Cuthbert, S.J.; Hursthouse, A.S. Evaluation of hydrochemical characteristics and flow directions of groundwater quality in Udi Local Government Area Enugu State, Nigeria. *Environ. Earth Sci.* **2015**, *73*, 4541–4555. [[CrossRef](#)]
14. Wannous, M.; Jahnke, C.; Troeger, U.; Falk, M.; Bzuer, F. Hydrochemistry and environmental isotopes (^{18}O , ^2H , ^3H , $^3\text{He}/^4\text{He}$) of groundwater and floodwater in the great area of Hurgada, Eastern Desert of Egypt. *Environ. Earth Sci.* **2021**, *80*, 407. [[CrossRef](#)]
15. Guo, L.; Wang, G.; Sheng, Y.; Shi, Z.; Sun, X. Groundwater microbial communities and their connection to hydrochemical environment in Golmud, Northwest China. *Sci. Total Environ.* **2019**, *695*, 133848. [[CrossRef](#)]
16. Li, Y.; Wu, P.; Huang, X.; Zhang, B.; Xu, Z.; Li, Y.; Li, J.; Wang, L.; Sun, Y.; Meng, X.; et al. Groundwater sources, flow patterns, and hydrochemistry of the Central Yinchuan Plain, China. *Hydrogeol. J.* **2021**, *29*, 591–606. [[CrossRef](#)]
17. Zhang, Y.; Shen, Y.; Chen, Y.; Wang, Y. Spatial characteristics of surface water and groundwater using water stable isotope in the Tarim River Basin, northwestern China. *Ecohydrology* **2013**, *6*, 1031–1039. [[CrossRef](#)]
18. Liu, J.; Wang, M.; Gao, Z.; Chen, Q.; Wu, G.; Li, F. Hydrochemical characteristics and water quality assessment of groundwater in the Yishu River basin. *Acta Geophys.* **2020**, *68*, 877–889. [[CrossRef](#)]
19. Piper, A.M. A graphic procedure in the geochemical interpretation of water-analyses. *Eos Trans. AGU* **1944**, *25*, 914–928. [[CrossRef](#)]
20. Wang, H.; Ni, J.; Song, Q.; Li, C.; Wang, F.; Cao, Y. Analysis of coastal groundwater hydrochemistry evolution based on groundwater flow system division. *J. Hydrol.* **2021**, *601*, 126631. [[CrossRef](#)]
21. Zhai, Y.; Zheng, F.; Zhao, X.; Xia, X.; Teng, Y. Identification of hydrochemical genesis and screening of typical groundwater pollutants impacting human health: A case study in Northeast China. *Environ. Pollut.* **2019**, *252*, 1202–1215. [[CrossRef](#)]
22. Liu, F.; Qian, H.; Shi, Z.; Wang, H. Long-term monitoring of hydrochemical characteristics and nitrogen pollution in the groundwater of Yinchuan area, Yinchuan basin of northwest China. *Environ. Earth Sci.* **2019**, *78*, 700. [[CrossRef](#)]
23. Chen, J.; Qian, H.; Gao, Y.; Wang, H.; Zhang, M. Insights into hydrological and hydrochemical processes in response to water replenishment for lakes in arid regions. *J. Hydrol.* **2020**, *581*, 124386. [[CrossRef](#)]
24. Li, P.; He, S.; He, X.; Tian, R. Seasonal hydrochemical characterization and groundwater quality delineation based on matter element extension analysis in a paper wastewater irrigation area, northwest China. *Expo. Health* **2018**, *10*, 241–258. [[CrossRef](#)]
25. Zhu, G.; Su, Y.; Feng, Q. The hydrochemical characteristics and evolution of groundwater and surface water in the Heihe River Basin, northwest China. *Hydrogeol. J.* **2008**, *16*, 167–182. [[CrossRef](#)]
26. Sun, C.; Li, X.; Chen, Y.; Li, W.; Stotler, R.L.; Zhang, Y. Spatial and temporal characteristics of stable isotopes in the Tarim River Basin. *Isot. Environ. Health Stud.* **2016**, *52*, 281–297. [[CrossRef](#)]
27. Sun, C.; Li, W.; Chen, Y.; Li, X.; Yang, Y. Isotopic and hydrochemical composition of runoff in the Urumqi River, Tianshan Mountains, China. *Environ. Earth Sci.* **2015**, *74*, 1521–1537.
28. Chen, H.; Chen, Y.; Li, W.; Hao, X.; Li, Y.; Zhang, Q. Identifying evaporation fractionation and streamflow components based on stable isotopes in the Kaidu River Basin with mountain–oasis system in north-west China. *Hydrol. Processes* **2018**, *32*, 2423–2434.
29. Cooper, R.J.; Hiscock, K.M.; Lovett, A.A.; Dugdale, S.J.; Sünnerberg, G.; Vrain, E. Temporal hydrochemical dynamics of the River Wensum, UK: Observations from long-term high-resolution monitoring (2011–2018). *Sci. Total Environ.* **2020**, *724*, 138253. [[CrossRef](#)]
30. Li, Z.; Feng, Q.; Wang, Q.; Kong, Y.; Cheng, A.; Song, Y.; Li, Y.; Li, J.; Guo, X. Contributions of local terrestrial evaporation and transpiration to precipitation using $\delta^{18}\text{O}$ and D-excess as a proxy in Shiyang inland river basin in China. *Glob. Planet. Chang.* **2016**, *146*, 140–151.
31. Li, Z.; Feng, Q.; Wang, Q.; Song, Y.; Li, H.; Li, Y. The influence from the shrinking cryosphere and strengthening evapotranspiration on hydrologic process in a cold basin, Qilian Mountains. *Glob. Planet. Chang.* **2016**, *144*, 119–128.
32. Wei, H.; Xu, Z.; Liu, H.; Ren, J.; Fan, W.; Lu, N.; Dong, X. Evaluation on dynamic change and interrelations of ecosystem services in a typical mountain-oasis-desert region. *Ecol. Indic.* **2018**, *93*, 917–929. [[CrossRef](#)]
33. Fu, Q.; Hou, Y.; Wang, B.; Bi, X.; Bo, L.; Zhang, X. Scenario analysis of ecosystem service changes and interactions in a mountain-oasis-desert system: A case study in Altay Prefecture, China. *Sci. Rep.* **2018**, *8*, 12939. [[CrossRef](#)]
34. Mamat, Z.; Haximu, S.; Zhang, Z.; Aji, R. An ecological risk assessment of heavy metal contamination in the surface sediments of Bosten Lake, northwest China. *Environ. Sci. Pollut. Res.* **2016**, *23*, 7255–7265. [[CrossRef](#)] [[PubMed](#)]
35. Wang, S.; Wu, B.; Yang, P. Assessing the changes in land use and ecosystem services in an oasis agricultural region of Yanqi Basin, Northwest China. *Environ. Monit. Assess.* **2014**, *186*, 8343–8357. [[CrossRef](#)]

36. Yao, J.; Chen, Y.; Zhao, Y.; Yu, X. Hydroclimatic changes of Lake Bosten in Northwest China during the last decades. *Sci. Rep.* **2018**, *8*, 9118. [[CrossRef](#)]
37. Zheng, L.; Xia, Z.; Xu, J.; Chen, Y.; Yang, H.; Li, D. Exploring annual lake dynamics in Xinjiang (China): Spatiotemporal features and driving climate factors from 2000 to 2019. *Clim. Chang.* **2021**, *166*, 36. [[CrossRef](#)]
38. Lei, X.; Lu, J.; Liu, Z.; Tong, Y.; Li, S. Concentration and distribution of antibiotics in water–sediment system of Bosten Lake, Xinjiang. *Environ. Sci. Pollut. Res.* **2015**, *22*, 1670–1678. [[CrossRef](#)]
39. Li, Y.; Ye, Q. Climate classification over China based on Köppen climate classification in the context of ENSO. *Clim. Chang. Res.* **2019**, *15*, 352.
40. Wang, T.; Zhou, D.; Shen, X. Spatial-temporal variations of Köppen climate types in China. *Terr. Atmos. Ocean. Sci.* **2021**, *32*, 483–496. [[CrossRef](#)]
41. Ba, W.; Du, P.; Liu, T.; Bao, A.; Chwn, X.; Liu, J.; Qin, C. Impacts of climate change and agricultural activities on water quality in the Lower Kaidu River Basin, China. *J. Geogr. Sci.* **2020**, *30*, 164–176. [[CrossRef](#)]
42. Asadi, E.; Isazadeh, M.; Samadianfard, S.; Ramli, M.F.; Mosavi, A.; Nabipour, N.; Shamsirband, S.; Hajnal, E.; Chau, K.W. Groundwater quality assessment for sustainable drinking and irrigation. *Sustainability* **2019**, *12*, 177. [[CrossRef](#)]
43. Liu, W.; Ma, L.; Abuduwaili, J.; Lin, L. Distributions, Relationship and Assessment of Major Ions and Potentially Toxic Elements in Waters of Bosten Lake, the Former Largest Inland and Freshwater Lake of China. *Water* **2020**, *2*, 2859. [[CrossRef](#)]
44. Li, D.; Chen, H.; Jia, S.; Lv, A. Possible Hydrochemical Processes Influencing Dissolved Solids in Surface Water and Groundwater of the Kaidu River Basin, Northwest China. *Water* **2020**, *2*, 467. [[CrossRef](#)]
45. Zhang, B.; Zhao, D.; Zhou, P.; Qu, S.; Liao, F.; Wang, G. Hydrochemical characteristics of groundwater and dominant water-rock interactions in the Delingha Area, Qaidam Basin, Northwest China. *Water* **2020**, *12*, 836. [[CrossRef](#)]
46. Feng, X.; Yang, Y. Hydrochemical and stable isotopic spatiotemporal variation characteristics and their environmental significance in the Kashi River Mountain Area of Ili, Xinjiang, China. *Environ. Geochem. Health* **2022**, *44*, 799–816. [[CrossRef](#)]
47. Gao, Z.; Han, C.; Yuan, S.; Liu, J.; Peng, Y.; Li, C. Assessment of the hydrochemistry, water quality, and human health risk of groundwater in the northwest of Nansi Lake Catchment, north China. *Environ. Geochem. Health* **2022**, *44*, 961–977. [[CrossRef](#)] [[PubMed](#)]
48. Karunanidhi, D.; Aravinthasamy, P.; Deepali, M.; Subramani, T.; Bellows, B.C.; Li, P. Groundwater quality evolution based on geochemical modeling and aptness testing for ingestion using entropy water quality and total hazard indexes in an urban-industrial area (Tiruppur) of Southern India. *Environ. Sci. Pollut. Res.* **2021**, *28*, 18523–18538. [[CrossRef](#)]
49. Yuan, R.; Wang, M.; Wang, S.; Song, X. Water transfer imposes hydrochemical impacts on groundwater by altering the interaction of groundwater and surface water. *J. Hydrol.* **2020**, *583*, 124617. [[CrossRef](#)]
50. Yan, H.; Xiao, J.; Liu, T.; Liu, Y. Evaluation of groundwater geochemical characteristics and quality in the central and Northern Shaanxi Province, China. *Acta Geochim.* **2020**, *39*, 733–740. [[CrossRef](#)]
51. Vaiphei, S.P.; Kurakalva, R.M.; Sahadevan, D.K. Water quality index and GIS-based technique for assessment of groundwater quality in Wanaparthy watershed, Telangana India. *Environ. Sci. Pollut. Res.* **2020**, *27*, 45041–45062. [[CrossRef](#)] [[PubMed](#)]
52. Feng, W.; Qian, H.; Xu, P.; Hou, K. Hydrochemical characteristic of groundwater and its impact on crop yields in the Baojixia irrigation area, China. *Water* **2020**, *12*, 1443. [[CrossRef](#)]
53. Li, P.; Li, X.; Meng, X.; Li, M.; Zhang, Y. Appraising groundwater quality and health risks from contamination in a Semiarid region of Northwest China. *Expos. Health* **2016**, *8*, 361–379. [[CrossRef](#)]
54. Zhang, Q.; Xu, P.; Qian, H.; Yang, F. Hydrogeochemistry and fluoride contamination in Jiaokou Irrigation District, Central China: Assessment based on multivariate statistical approach and human health risk. *Sci. Total Environ.* **2020**, *741*, 140460. [[CrossRef](#)]
55. Wu, J.; Sun, Z. Evaluation of shallow groundwater contamination and associated human health risk in an alluvial plain impacted by agricultural and industrial activities, mid-west China. *Expo. Health* **2016**, *8*, 311–329. [[CrossRef](#)]
56. Liu, X.; Wang, X.; Zhang, L.; Fan, W.; Yang, C.; Li, E.; Wang, Z. Impact of land use on shallow groundwater quality characteristics associated with human health risks in a typical agricultural area in Central China. *Environ. Sci. Pollut. Res.* **2021**, *28*, 1712–1724. [[CrossRef](#)]
57. Chen, Y.; Li, B.; Fan, Y.; Sun, C.; Fang, G. Hydrological and water cycle processes of inland river basins in the arid region of Northwest China. *J. Arid Land* **2019**, *11*, 161–179. [[CrossRef](#)]
58. Zhang, Z.; Jia, W.; Zhu, G.; Shi, Y.; Yang, L.; Xiong, H.; Zhang, M.; Zhang, F. Hydrochemical characteristics and ion sources of river water in the upstream of the Shiyang River, China. *Environ. Earth Sci.* **2021**, *80*, 614. [[CrossRef](#)]
59. Guo, X.; Feng, Q.; Liu, W.; Li, Z.; Wen, X.; Si, J.; Xi, H.; Guo, R.; Jia, B. Stable isotopic and geochemical identification of groundwater evolution and recharge sources in the arid Shule River Basin of Northwestern China. *Hydrol. Process.* **2015**, *29*, 4703–4718. [[CrossRef](#)]
60. Wu, W. Hydrochemistry of inland rivers in the north Tibetan Plateau: Constraints and weathering rate estimation. *Sci. Total Environ.* **2016**, *541*, 468–482. [[CrossRef](#)]
61. Zhang, J.; Zhou, J.; Zhou, Y.; Zeng, Y.; Ji, Y.; Sun, Y.; Lei, M. Hydrogeochemical characteristics and groundwater quality assessment in the plain area of Yarkant River Basin in Xinjiang, PR China. *Environ. Sci. Pollut. Res.* **2021**, *28*, 31704–31716. [[CrossRef](#)] [[PubMed](#)]